frontiers | Frontiers in Medicine

Check for updates

Novel PET Imaging of Inflammatory Targets and Cells for the Diagnosis and Monitoring of Giant Cell Arteritis and Polymyalgia Rheumatica

Kornelis S. M. van der Geest[1], Maria Sandovici[1], Pieter H. Nienhuis[2], Riemer H. J. A. Slart[2,3], Peter Heeringa[4], Elisabeth Brouwer[1] and William F. Jiemy[1]*

[1] Department of Rheumatology and Clinical Immunology, University of Groningen, University Medical Center Groningen, Groningen, Netherlands, [2] Department of Nuclear Medicine and Molecular Imaging, Medical Imaging Center, University Medical Center Groningen, University of Groningen, Groningen, Netherlands, [3] Department of Biomedical Photonic Imaging Group, University of Twente, Enschede, Netherlands, [4] Department of Pathology and Medical Biology, University of Groningen, University Medical Center Groningen, Groningen, Netherlands

Giant cell arteritis (GCA) and polymyalgia rheumatica (PMR) are two interrelated inflammatory diseases affecting patients above 50 years of age. Patients with GCA suffer from granulomatous inflammation of medium- to large-sized arteries. This inflammation can lead to severe ischemic complications (e.g., irreversible vision loss and stroke) and aneurysm-related complications (such as aortic dissection). On the other hand, patients suffering from PMR present with proximal stiffness and pain due to inflammation of the shoulder and pelvic girdles. PMR is observed in 40–60% of patients with GCA, while up to 21% of patients suffering from PMR are also affected by GCA. Due to the risk of ischemic complications, GCA has to be promptly treated upon clinical suspicion. The treatment of both GCA and PMR still heavily relies on glucocorticoids (GCs), although novel targeted therapies are emerging. Imaging has a central position in the diagnosis of GCA and PMR. While [18F]fluorodeoxyglucose (FDG)-positron emission tomography (PET) has proven to be a valuable tool for diagnosis of GCA and PMR, it possesses major drawbacks such as unspecific uptake in cells with high glucose metabolism, high background activity in several non-target organs and a decrease of diagnostic accuracy already after a short course of GC treatment. In recent years, our understanding of the immunopathogenesis of GCA and, to some extent, PMR has advanced. In this review, we summarize the current knowledge on the cellular heterogeneity in the immunopathology of GCA/PMR and discuss how recent advances in specific tissue infiltrating leukocyte and stromal cell profiles may be exploited as a source of novel targets for imaging. Finally, we discuss prospective novel PET radiotracers that may be useful for the diagnosis and treatment monitoring in GCA and PMR.

Keywords: PET/CT, giant cell arteritis (GCA), polymyalgia rheumatica (PMR), radiotracer, imaging, large-vessel vasculitis (LVV)

INTRODUCTION

Giant cell arteritis (GCA) and polymyalgia rheumatica (PMR) are two related inflammatory diseases exclusively affecting adults above the age of 50, with a peak incidence between 75 and 79 years of age (1). GCA is a vasculitis affecting medium- to large-sized arteries which can be subclassified into a spectrum that includes cranial GCA (C-GCA) and large-vessel GCA (LV-GCA) (2). C-GCA mainly affects the cranial arteries and leads to ischemic symptoms such as jaw claudication, vision loss, and stroke (3, 4). LV-GCT mainly affects the aorta and its main branches and may lead to aneurysm formation and aortic dissection. Up to 83% of GCA patients present with overlapping C-GCA and LV-GCA (5). PMR is a rheumatic inflammatory disorder characterized by inflammation of bursae, tendon sheaths, and joints primarily affecting the shoulder and pelvic girdles (6). GCA and PMR commonly coexist; up to 60% of GCA patients are diagnosed with PMR while up to 21% of PMR patients present with overlapping GCA (7). To date, glucocorticoid (GC) therapy remains the mainstream treatment for the management of GCA and PMR (8). Although GC treatment is effective in inducing and maintaining remission, it can cause substantial toxicity in patients (9). Recently, IL-6 receptor blocking therapy has shown positive results as GC sparing therapy in GCA (10). Promising results with this therapy have also been reported in PMR (11, 12). However, tocilizumab monotherapy is not recommended for these diseases and combination treatment with GC is still imperative, especially in GCA.

Historically, the diagnosis of GCA solely relied on the assessment of clinical signs and symptoms, laboratory assessment of inflammatory markers such as elevated C-reactive protein (CRP) and erythrocyte sedimentation rate (ESR), and positive histological evidence of giant cell arteritis in the temporal artery biopsy (TAB) (13). Similarly, diagnosis of PMR also relies heavily on the assessment of clinical signs and symptoms, and laboratory assessment of inflammatory markers (14). More recently, imaging techniques such as ultrasonography and [18F]fluorodeoxyglucose (FDG)-positron emission tomography (PET) have gained importance as diagnostic tools for GCA and PMR, whereas these imaging techniques are also increasingly used for treatment monitoring (11, 15–18). Previously, [18F]FDG-PET/CT was only utilized for the detection of LV-GCA due to its limitation in resolution. However, [18F]FDG-PET/CT employing new generation scanners with improved resolution has been shown to be able to detect C-GCA. Recent reports have shown that C-GCA can be effectively detected by PET/CT (up to 83% sensitivity and 100% specificity) (19, 20). However, despite its utility, there are several important clinical drawbacks posed by [18F]FDG-PET as a diagnostic tool in the diagnosis of GCA and PMR. Firstly, [18F]FDG uptake is non-specific and only indicates increased glucose metabolism. Therefore, it may be present in the context of neoplasia, inflammation, degenerative disease, and increased muscle use (21). In the context of vascular inflammation, [18F]FDG may also be taken up due to atherosclerotic activity (21). In addition, [18F]FDG shows intense uptake in several

organs that may hamper its diagnostic accuracy. One example is the high brain uptake of [18F]FDG that may result in a low target-to-background ratio (TBR) in cranial vessels and limit the diagnostic accuracy of C-GCA. Furthermore, the diagnostic accuracy of [18F]FDG-PET in patients undergoing GC treatment is significantly reduced as exemplified by one study reporting that only 36% of LV-GCA patients showed a positive [18F]FDG-PET scan after 10 days of GC treatment (22). A reduction in diagnostic accuracy has also been shown in PMR patients undergoing GC treatment albeit to a lesser extent as compared to GCA (17). GC rapidly blocks glycolysis pathways important for FDG uptake in inflammatory cells (23, 24). It is imperative to start GC treatment upon suspicion of GCA while postponing the GC treatment can be difficult in patients with suspected PMR. Unfortunately, diagnostic imaging of these patients is often not feasible within a narrow timeframe due to limited hospital capacities. Therefore, there is a strong clinical need to identify novel radiotracers that (1) have low background radioactivity in non-target organs and blood pool, and (2) can still accurately detect ongoing inflammation for a prolonged period (e.g., up to weeks) after initiation of GC treatment. Such radiotracers could potentially help to firmly rule in or rule out GCA/PMR and would provide an important benefit to patients in which the diagnosis remains uncertain despite routine clinical evaluation. With the expanding knowledge regarding the cellular heterogeneity at the site of inflammation in GCA and PMR, novel radiotracers targeting these specific cell subsets may prove to be useful for the diagnosis and eventually treatment monitoring in GCA and PMR patients.

IMMUNOPATHOLOGY OF GCA AND PMR

C-GCA

The immunopathology of GCA is characterized by leukocyte infiltration at the site of inflammation. Although not yet fully understood, decades of efforts in characterizing and understanding the cellular heterogeneity in the inflamed GCA vessels have led us to better understand the pathogenesis of this disease. Based on these data, a pathogenic model has been established in which the initiation of GCA is believed to start with the activation of vascular dendritic cells (vasDCs) through toll-like receptors (TLRs) stimulation by still unknown triggers. Upon activation, these vasDCs adopt a phenotype characterized by the expression of the activation marker CD83 and elevated expression of the costimulatory molecule CD86 (25). These activated vasDCs express the chemokines CCL19 and CCL21 while simultaneously expressing the receptor CCR7, causing these activated vasDCs to be trapped in the vessel wall. Moreover, these activated vasDCs produce CCL20 and a range of proinflammatory cytokines (IL-1β, IL-6, IL-18, IL-23, and IL-33) leading to the recruitment of CD4+ T cells into the vessel-wall, their subsequent co-stimulation and activation, and their polarization into Th1 and Th17 cells (26–29). Although infiltrating T cells in the vessel wall show expression of the inhibitory checkpoint molecule PD-1, vasDCs exhibit low expression of the coinhibitory ligand PD-L1 resulting in dampened negative regulation of T cell activation (30,

31). Activated Th1 and Th17 cells produce high amounts of IFNγ and IL-17, respectively, which in turn activate the resident vascular smooth muscle cells (VSMCs) and endothelial cells (ECs). Activated ECs express high levels of adhesion molecules (VCAM-1, ICAM-1 and E-selectin) enabling leukocyte adhesion and transmigration to the vessel wall (32). Activated VSMCs produce several crucial chemokines such as CXCL9, CXCL10, CXCL11, CXCL13, CCL2, and CX3CL1 augmenting the infiltration of CXCR3+ CD8+ T cells, CXCR3+/CXCR5+ B cells, and CCR2+/CX3CR1+ monocytes to the vessel wall (33–37). Infiltrating CD20+ B cells organize themselves into tertiary lymphoid organs (TLOs) where they produce proinflammatory cytokines which perpetuate the inflammatory processes (38, 39). Infiltrating CD8+ T cells start to produce cytokines such as IFN-γ and IL-17 which triggers a positive feedback loop recruiting more CD4+ and CD8+ T cells as well as monocytes to the vessel wall (36). Notably, activated VSMCs, ECs, CD4+ and CD8+ T cells also produce GM-CSF, a potent hematopoietic growth factor that induces the differentiation and maturation of infiltrating monocytes into proinflammatory CD206+ macrophages (40, 41). These CD206+ macrophages express the collagenase matrix metalloproteinase (MMP)-9 and proangiogenic factor YKL-40 (42). These CD206+/YKL-40+/MMP-9+ macrophages are mainly located in the media and media borders promoting collagen degradation and neovessel formation, enabling more invasion of T cells and monocytes into the vessel wall (42–45). In addition, these CD206+ macrophages express high levels of the growth factor M-CSF, priming adjacent macrophages to become FRβ+ macrophages (41). These M-CSF primed FRβ+ macrophages produce high levels of platelet-derived growth factor (PDGF)-AA which promotes fibroblast migration and proliferation. Furthermore, macrophages are incredibly plastic cells that may change their phenotype in response to cues from the microenvironment. Proinflammatory cytokines such as IFNγ, IL-17, and IL-6 that are abundantly present in the inflamed vessel wall may trigger the expression of a multitude of macrophage markers (5). Notably, abundant numbers of CD64+, CD86+, iNOS+ and CD163+ macrophages have been reported in GCA-affected vessels (41, 46–48). Moreover, these activated macrophages themselves produce a wide range of proinflammatory cytokines (including IL-6, TNF-α, IL-1β, GM-CSF) and growth factors (TGF-β, VEGF, PDGFs) (5). Macrophage secreted proinflammatory cytokines contribute to a positive feedback loop amplifying the inflammatory process. Macrophage secreted growth factors promote fibroblasts and VSMCs activation and differentiation into α-smooth muscle actin (SMA)+ myofibroblasts and subsequently their migration and proliferation in the intima layer which results in intimal hyperplasia and ultimately vessel-wall occlusion (49, 50). Of note, this pathogenic model has largely been constructed from studies on TAB obtained from C-GCA patients.

LV-GCA

Our understanding of the pathogenesis of LV-GCA is derived from studies with aortic specimens obtained during aortic aneurysm surgery. Aortitis in GCA is characterized by granulomatous inflammation largely occurring in the medial layer of the aorta. This granulomatous inflammation leads to medial necrosis which is responsible for aortic aneurysm and may ultimately lead to aortic dissection. Although the final consequences of LV-GCA may differ from C-GCA, the cellular infiltrates are largely similar. Infiltrating leukocytes in the inflamed aorta largely dominate the adventitia and the media layer of the aorta. Infiltration of both activated CD4+ and CD8+ T cells has been reported in GCA affected aorta (51). While the infiltration of T cells in adventitia and media of the aorta has been described, infiltration of CD20+ B cells mainly localizes in the adventitia where these cells are organized into TLOs (38). Macrophages expressing CD64, CD86, CD206, and FRβ are abundant in the adventitia and the media of GCA-affected aortas (41). CD206+/MMP-9+/YKL-40+ macrophages surround the necrotic areas in the media indicating a role in medial destruction (41). Notably, a reduction of α-SMA+ cells has been reported in the media of GCA-affected aortas due to medial necrosis which differs from the increase of adventitial and intimal α-SMA+ myofibroblasts in temporal arteries (52).

PMR

In contrast to GCA, not much is currently known regarding the immunopathology of PMR. One of the first reports studying synovial tissue biopsies of PMR patients was published in 1964 in which hyperplasia of synovial lining cells, increased vascularity, and leukocyte infiltration mainly consisting of lymphocytes and macrophages were described (53). In the 1990s, immunohistological investigation on glenohumeral synovial tissue of patients with PMR revealed that CD68+ macrophages comprise the majority of the infiltrating cells followed by T cells and a small percentage of neutrophils (54). The T cell infiltrates were mainly comprised of CD45RO+ memory CD4+ T cells although small numbers of CD8+ T cells were also detected. B cells were not detected in the synovial tissue. In another report, the same group showed elevated VEGF expression by both CD3+ T cells and CD68+ macrophages in synovial biopsy tissues which correlated with vessel density indicating that these cells are involved in vasa vasorum formation and subsequently enhanced leukocyte infiltration in the synovium of PMR patients (55). More recently, enrichment of both CD4+ and CD8+ T cells in the synovial fluid of PMR patients have been reported (56). These T cells show a high IFNγ producing capacity pointing toward Th1 and Tc1 subsets. To date, no further cellular profiling has been done in the synovial tissues of PMR patients. Taking clues from other inflammatory diseases of the joint such as rheumatoid arthritis (RA) and osteoarthritis (OA), infiltration of CD206+, FRβ+, CD163+, MMP-9+ and iNOS+ macrophages has been reported (57, 58). Whether or not these cells are also involved in the immunopathology of PMR remains to be elucidated. Therefore, it is warranted for future studies to focus on deeper phenotyping of the cellular infiltrates in PMR synovial biopsies to better understand their roles in the immunopathology of PMR and subsequently target these cells for imaging and therapeutic purposes.

POTENTIAL NOVEL PET TRACERS FOR DIAGNOSIS AND MONITORING OF GCA AND PMR

The knowledge regarding the cellular heterogeneity in the pathogenesis of GCA and PMR may allow us to target these specific cells for imaging purposes. For a long time, [^{18}F]FDG-PET has dominated the imaging landscape in oncology and inflammatory diseases alike. However, more recent efforts have shifted the trend toward targeting a specific cellular population. Targeting specific cell populations may provide the following advantages compared to [^{18}F]FDG-PET:

(1) Lower background activity, thereby increasing target-to-background ratio and the imaging accuracy.

(2) Ability to evaluate specific cell populations as prognostic markers for disease progression and treatment response, thereby aiding the design of personalized treatment regimens, especially with emerging novel immunotherapies.

(3) Better insight into treatment effects. Novel immunotherapies often specifically target cellular pathways which may alter specific cell populations at the site of inflammation.

(4) Cellular infiltrates are unlikely to disappear immediately upon initiation of treatments in patients with immune-mediated inflammatory diseases including GCA and PMR (54, 59, 60), whereas especially glucocorticoid treatment may promptly impact the glucose metabolism by infiltrating immune cells and liver. Thus, the time interval of diagnostic scanning for cell-specific PET tracers might potentially be longer.

As the efforts in developing PET radiotracers targeting specific cell populations are increasing, these radiotracers may also prove to be useful for the imaging of GCA and PMR which is summarized below (**Figure 1**).

T Cell-Targeted Radiotracers

T cells are one of the most abundant infiltrating cell types in the inflamed GCA vessels (61). In the synovium of PMR patients, although not the most abundant cells, infiltration of T cells has been documented as well (54). Several radiotracers targeting T cells have been developed and are currently undergoing clinical trials for imaging other diseases, primarily oncology (**Table 1**). These radiotracers may also prove to be useful for the imaging of GCA and PMR patients.

IL-2 is a pleiotropic cytokine highly secreted by activated T cells which promotes T cell survival, expansion and differentiation into effector cells (72). The IL-2 receptor consists of three subunits including IL-2Rα (CD25), IL-2Rβ (CD122), and IL-2Rγ (CD132). IL-2 signals through the intermediary IL-2 receptor comprising the IL-2Rβ and IL-2Rγ chain. Upon activation, T cells gain elevated expression of CD25, completing the high-affinity receptor with the three subunits (72, 73). As a crucial cytokine in T cell functions, IL-2 is rapidly consumed by activated T cells making it an attractive cytokine for targeted imaging of activated T cells. The IL-2 targeted SPECT radiotracers, [^{99m}Tc]IL-2 and [^{99m}Tc]HYNIC-IL-2, have already been applied successfully for the visualization of vulnerable atherosclerotic plaques, transplant rejection and autoimmune thyroid disease (74–76). Furthermore, visualization of Takayasu arteritis has been reported in a case study utilizing [^{99m}Tc]IL-2 scintigraphy (77), pointing toward the possible utility of IL-2 based lymphocyte targeted imaging in the detection of GCA.More recently, several PET radiotracers based on radionuclide tagged IL-2 have been reported. The first-generation IL-2 tracer, [^{18}F]FB-IL-2, was reported to show high-affinity binding to activated human peripheral blood mononuclear cells (hPBMCs). The reports showed a high correlation of [^{18}F]FB-IL-2 uptake with the number of CD25+ cells *in vitro* and in matrigel implants with activated hPBMCs (62–64). In a recent study, [^{18}F]FB-IL-2 imaging successfully detected tumor lesions in metastatic melanoma patients (63). Biodistribution data showed high uptake in secretion organs (liver and kidneys), lymphoid organs (spleen and bone marrow) and the blood pool (myocardial and aortic) but low uptake in other non-target organs including the brain. The high blood pool radioactivity, however, may mask the detection of arterial inflammation in GCA. Recently, second-generation IL-2 based tracers, [^{18}F]AIF-RESCA-IL2 and [^{68}Ga]Ga-NODAGA-IL2 have been developed (65). Although yet to be tested in humans, both radiotracers showed high specific uptake in lymphoid tissue and hPBMC xenografts in a mouse model. In addition, both second-generation radiotracers showed no brain uptake and lower blood pool radioactivity compared to [^{18}F]FB-IL-2 which may be advantageous for the detection of aortic and arterial inflammation in GCA. Furthermore, as T cell infiltration in the synovium of PMR patients has been documented, these radiotracers may also prove to be useful for PMR imaging.

Dominant CD4+ T cell infiltration over CD8+ T cells at the site of inflammation has been reported for both GCA and PMR (51, 54), making CD4+ T cells an attractive target for imaging of these diseases. Two ImmunoPET tracers targeting human CD4 T cells have been recently reported. Nanobody-based [^{64}Cu]CD4-Nb1 showed specific uptake in organs with high numbers of CD4+ T cells including lymph nodes, thymus, spleen, and liver with rapid blood and lung clearance *via* renal elimination in a human CD4 knock-in mouse model (66). Similarly, minibody based [^{64}Cu]NOTA-IAB41 showed specific uptake in CD4+ T cells infiltrated lungs, spleen, liver and kidney in hPBMC injected humanized mice (67). Interestingly, the report also showed successful visualization of CD4+ T cell infiltration in a humanized brain tumor mouse model compared to no brain uptake in the non-disease control group. Both radiotracers may potentially be useful in imaging GCA and PMR patients.

Lower numbers of infiltrating CD8+ T cells compared to CD4+ T cells have been reported in the inflamed vessels of GCA patients. However, CD8 targeted imaging may still be valuable for this disease since the presence of large arterial CD8 T cell infiltrates is associated with disease severity (51). A minibody based CD8+ T cell-targeted radiotracer, [^{89}Zr]Df-IAB22M2C, has been developed and is currently actively investigated in several clinical trials. Reports of CD8+ T cells imaging in patients with solid tumors have shown successful visualization of tumor-infiltrating CD8+ T cells and specific uptake in CD8+ rich lymphoid organs (70, 71). Moreover, low blood pool radioactivity
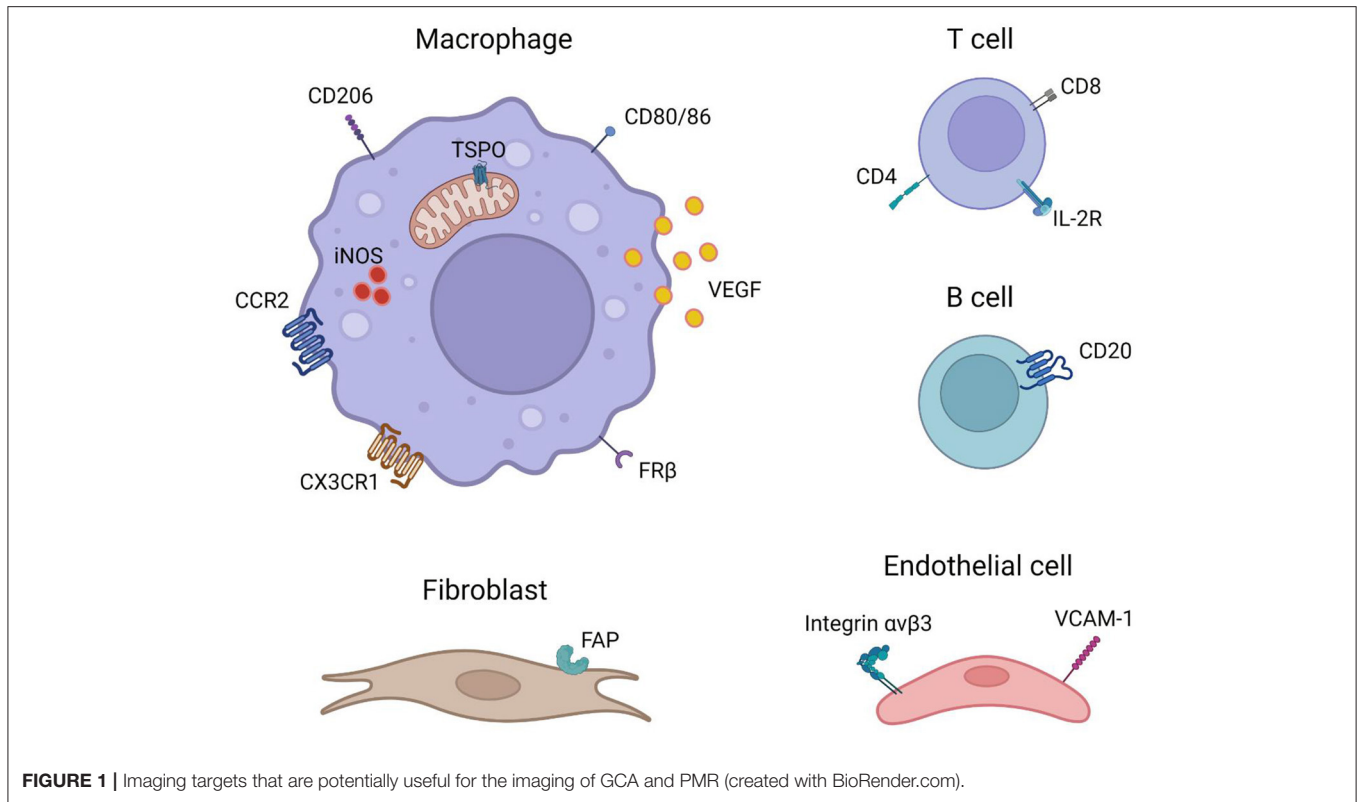
FIGURE 1 | Imaging targets that are potentially useful for the imaging of GCA and PMR (created with BioRender.com).

TABLE 1 | T cell targeted PET radiotracers.

Target cell	Target marker/ pathway	Radiotracer	Class	Clinical/ preclinical	Active clinical trials	References
Activated T cells	IL-2R	[^{18}F]FB-IL-2	Cytokine	Clinical	NCT04163094 NCT02478099	(62–64)
	IL-2R	[^{18}F]AIF-RESCA-IL2	Cytokine	Preclinical	–	(65)
	IL-2R	[^{68}Ga]Ga-NODAGA-IL2	Cytokine	Preclinical	–	(65)
CD4+ T cells	CD4 molecule	[^{64}Cu]CD4-Nb1	Nanobody	Preclinical	–	(66)
		[^{64}Cu]NOTA-IAB41	Minibody	Preclinical	–	(67)
CD8+ T cells	CD8 molecule	[^{89}Zr]-Df-IAB22M2C	Minibody	Clinical	NCT03802123 NCT04874818 NCT04826393 NCT05013099 NCT04606316 NCT04180215 NCT03533283	(68–71)

and no brain uptake were detected in these patients making it suitable for imaging C-GCA and LV-GCA. The infiltration of CD8+ T cells in the synovium of PMR patients is scarce and therefore CD8+ T cell-targeted imaging may be less suitable for PMR.

Although PD-1 expressing T cell infiltration has been reported in GCA (30, 31), only two radiotracers targeting PD-1 based on PD-1 antagonist nivolumab and pembrolizumab are currently available (78). Since the development of both GCA and PMR as consequences of PD-1/PD-L1 inhibition therapy of cancer patients has been reported (79, 80), the use of these radiotracers

for the imaging of GCA and PMR may potentially worsen the disease and is therefore not feasible. However, with the rise of PD-1 agonists (81–84), future applications of these PD-1 agonist-based radiotracers may prove to be useful as a theranostic approach in these diseases.

Macrophage Targeted Radiotracers

Macrophages play vital roles and are one of the most abundant cell types infiltrating the inflamed vessels and synovial tissue of GCA and PMR patients making them attractive targets for cell-specific imaging (5, 54). As macrophages are incredibly

plastic cells, not all tracers are suitable for the imaging of macrophages in GCA and PMR patients. As our knowledge regarding macrophage heterogeneity in the pathogenesis of GCA has improved considerably, we will focus on a selected number of radiotracers targeting macrophage phenotypes that have been proven to be involved in the vasculopathy of GCA (**Table 2**).

Macrophage-targeted imaging of translocator protein (TSPO; also known as PBR or peripheral benzodiazepine receptor) was first developed for the targeted imaging of microglia in neuroinflammation. It was later found that TSPO targeted imaging could be utilized for the imaging of non-neuronal inflammatory diseases such as rheumatoid arthritis (RA), atherosclerosis, Takayasu arteritis (TAK), systemic lupus erythematosus (SLE), and GCA (88, 94, 98–100, 103, 106, 185, 190, 193). In 2010, Pugliese et al. successfully showed the utility of [^{11}C]PK11195, a first-generation TSPO targeted radiotracer, in the detection of large-vessel vasculitis including GCA (94). Shortly after, another study led by Lamare et al. utilizing the radiotracer [^{11}C]-(R)-PK11195 showed a similar result in detecting vascular inflammation in patients suffering from large-vessel vasculitis (106). Additionally, studies have shown high uptake of a second-generation TSPO tracer, [^{11}C]DPA-713, in inflamed joints of RA patients pointing to the potential in imaging PMR (185, 193). Although the utility has been shown in imaging GCA, older generation TSPO targeted radiotracers possess several disadvantages. The major drawback of these radiotracers is the significantly lower binding capability to TSPO in patients with a common TSPO gene polymorphism (*rs6971*), which resulted in variability in the imaging signal (324, 325). Furthermore, these older generation TSPO targeted tracers are not very specific and show high background radioactivity, which may hamper the imaging capability (326). The third generation of TSPO targeted radiotracers, such as [^{18}F]FEBMP, [^{18}F]ER176 and [^{18}F]-(S)-GE387, are designed to overcome these drawbacks. Notably, a recent study using another second-generation tracer, [^{11}C]PBR28, documented no vascular uptake in patients suffering from large-vessel vasculitis (Takayasu arteritis and GCA) (327). It is unclear whether this discrepancy was caused by the unspecific binding of the first-generation TSPO tracers in the inflamed tissues. This discrepancy warrants a more detailed investigation into the feasibility of new generation TSPO targeted tracers in imaging GCA.

The mannose receptor (CD206) is a C-type lectin receptor highly expressed by certain populations of macrophages. Several CD206 targeted radiotracers have been developed and some have been used in clinical applications (**Table 2**). Employing the receptor-ligand binding approach, tracers based on mannose derivatives, mannose coated liposome, and mannosylated protein have shown reliable CD206 targeting. [^{18}F]FDM based on fluorodeoxy-mannose have been shown to have lower non-specific brain uptake compared to [^{18}F]FDG in patients with brain infarction (241). Furthermore, this radiotracer has been successfully used in preclinical imaging of atherosclerotic lesions in a rabbit model supporting its potential in vascular imaging (328). More recently, anti-CD206 nanobody-based radiotracers have been developed which are more specific compared to

the mannose derivatives-based tracers. In animal models of atherosclerosis and cancer, these radiotracers have shown rapid blood clearance and low radioactivity in non-target organs including the brain (243, 245, 246). The abundance of CD206+ macrophages responsible for expressing high levels of YKL-40 and MMP-9, a proangiogenic and tissue destructive collagenase, respectively, has been documented in affected vessels of GCA patients (41, 42). These macrophages are likely skewed by GM-CSF in the microenvironment and are considered to be responsible for media destruction in GCA. Given their prominent roles, targeted imaging of CD206+ macrophages may be beneficial for the diagnosis and prognosis of GCA.

The interest in folate-based imaging started over two decades ago when folate receptor-expressing tumors were discovered (329). This led to the rapid development of numerous folate receptor-targeted radiopharmaceuticals. Of note, some of these radiotracers are tagged with highly radioactive nuclides or toxic particles intended as radiotherapeutics for cancers (330–333). More recently, it has been demonstrated that some macrophages involved in autoimmune and inflammatory diseases, including GCA, express high levels of folate receptor beta (FRβ) as well. Interestingly, the degree of FRβ+ macrophage infiltration in the intima of the GCA affected vessels has been linked to intimal hyperplasia (41). Patients with intimal hyperplasia in their biopsy may be more likely to develop ischemic complications than those without (334). Imaging FRβ may potentially reveal the degree of vessel wall occlusion in C-GCA and may signal the need for the rapid induction of high-dose GC therapy to lower the risk of vision loss in these patients. Among the plethora of FR-targeted radiotracers, [^{18}F]fluoro-PEG-folate and [^{18}F]AzaFol have been used in clinical applications (259, 263). [^{18}F]fluoro-PEG-folate was assessed in patients with RA and showed specific uptake in inflamed joints with low brain uptake. The infiltration of FRβ+ macrophages in the synovial tissue of RA patients has been well-documented. On the other hand, the utility of [^{18}F]AzaFol was assessed in patients with FRα+ adenocarcinoma of the lungs. These studies demonstrate the utility of these novel folate receptor-targeted radiotracers in human subjects, but at the same time revealed that folate receptor imaging may not be very specific due to uptake by both FRα+ and FRβ+ cells. Nevertheless, folate receptor imaging may still prove to be useful in patients suffering from GCA especially in the detection of patients at risk of developing ischemic events due to severe intimal hyperplasia.

Immunotherapy targeting T cell activation by blocking CD80/86 on antigen-presenting cells (APCs) with a CTLA-4Ig fusion protein (abatacept) is currently evaluated in GCA (NCT04474847). An earlier phase II randomized control trial of abatacept for the treatment of GCA showed promising results with significant proportions of patients achieving relapse-free survival rate at 12 months compared to placebo (48% abatacept vs. 31% placebo; $p = 0.049$) (335). Separately, a case report has shown the potential application of abatacept for the treatment of PMR (336). Together, these encouraging results may point toward the potential application of radionuclide tagged [^{64}Cu]NODAGA-abatacept in GCA and PMR.

TABLE 2 | Macrophage targeted PET radiotracer.

Target marker/ pathway	Radiotracer	Class	Clinical/ preclinical	Active clinical trials	References
TSPO	[^{11}C]PK11195	TSPO antagonist	Clinical	NCT03368677 NCT04239820 NCT05111678	(85–94)
	[^{11}C]-(R)-PK11195	TSPO antagonist	Clinical	–	(95–114)
	[^{11}C]DAA1106	TSPO agonist	Clinical	–	(115–121)
	[^{18}F]DAA1106	TSPO agonist	Preclinical	–	(122–124)
	[^{18}F]FEDAA1106	TSPO agonist	Clinical	–	(125–130)
	[^{18}F]FMDAA1106	TSPO agonist	Preclinical	–	(125)
	[^{11}C]PBR28	TSPO agonist	Clinical	NCT04274998 NCT05205291 NCT04230174 NCT03705715 NCT04490096 NCT02649985 NCT04236986 NCT04398719 NCT04811404 NCT04066244 NCT04233593 NCT03106740 NCT05066308 NCT04486118 NCT05183087	(131–145)
	[^{18}F]PBR06	TSPO agonist	Clinical	NCT04510220 NCT03983252 NCT04144257 NCT02649985	(146–150)
	[^{11}C]PBR06	TSPO agonist	Preclinical	–	(147)
	[^{11}C]PBR01	TSPO agonist	Preclinical	–	(151, 152)
	[^{18}F]FEPPA	TSPO agonist	Clinical	NCT02945774 NCT04814355 NCT04307667 NCT04854785	(153–163)
	[^{18}F]PBR111	TSPO antagonist	Clinical	–	(164–169)
	[^{18}F]PBR102	TSPO antagonist	Preclinical	–	(166, 169, 170)
	[^{11}C]CB184	TSPO antagonist	Clinical	–	(171–174)
	[^{11}C]CLINME	TSPO ligand	Preclinical	–	(167, 175, 176)
	[^{18}F]CB251	TSPO ligand	Preclinical	–	(177–179)
	[^{11}C]AC-5216	TSPO agonist	Preclinical	–	(180)
	[^{11}C]DAC	TSPO agonist	Preclinical	–	(181, 182)
	[^{11}C]DPA-713	TSPO agonist	Clinical	–	(183–193)
	[^{18}F]DPA-714	TSPO agonist	Clinical	NCT03759522 NCT03754348 NCT03457493 NCT04362644 NCT03999164 NCT04364672 NCT04542603 NCT03230526 NCT03968445 NCT05238961 NCT04520802 NCT05147532 NCT03691077 NCT04171882 NCT03482115 NCT03314155	(193–195)

(Continued)

TABLE 2 | Continued

Target marker/ pathway	Radiotracer	Class	Clinical/ preclinical	Active clinical trials	References
				NCT05128903 NCT03435861 NCT05233605 NCT04785157	
	[^{18}F]DPA-C5yne	TSPO agonist	Preclinical	–	(196)
	[^{18}F]FDPA	TSPO agonist	Preclinical	–	(197–200)
	[^{18}F]VUIIS1018A	TSPO agonist	Preclinical	–	(201, 202)
	[^{18}F]FEDAC	TSPO ligand	Preclinical	–	(203–205)
	[^{11}C]SSR180575	TSPO agonist	Preclinical	–	(206)
	[^{18}F]SSR180575	TSPO agonist	Preclinical	–	(207)
	[^{18}F]FEMPA	TSPO ligand	Clinical	NCT05039268	(208–210)
	[^{18}F]FETEM	TSPO ligand	Preclinical	–	(211)
	[^{18}F]FEBMP	TSPO ligand	Preclinical	–	(212, 213)
	[^{18}F]GE180	TSPO ligand	Clinical	NCT04412187 NCT03702816	(214–223)
	(R)-[^{18}F]NEBIFQUINIDE	TSPO ligand	Preclinical	-	(224)
	[^{11}C]ER176	TSPO ligand	Clinical	NCT04762719 NCT04840979 NCT03705715 NCT04576793 NCT03958630 NCT03912428 NCT04510168 NCT04786548	(225–228)
	[^{18}F]ER176 analogs	TSPO ligand	Preclinical	–	(229, 230)
	[^{18}F]-(S)-GE387	TSPO ligand	Preclinical	–	(223, 231)
	[^{18}F]LW223	TSPO ligand	Preclinical	–	(232, 233)
	[^{18}F]BS224	TSPO ligand	Preclinical	–	(234)
CD206	[^{64}Cu]MAN-LIPs	Mannose coated liposome	Preclinical	–	(235)
	[^{68}Ga]NOTA-MSA	Mannosylated protein	Clinical	–	(236–239)
	[^{18}F]FDM	Mannose derivative	Clinical	–	(240, 241)
	[^{68}Ga]IRDye800-tilmanocept	Mannose derivative	Preclinical	–	(242)
	[^{18}F]FB-anti-MMR 3.49 sdAb	Nanobody	Preclinical	–	(243)
	[^{68}Ga]MMR	Nanobody	Preclinical	–	(244)
	[^{68}Ga]Ga-NOTA-anti-MMR-sdAb	Nanobody	Preclinical	–	(245)
	[^{68}Ga]Ga-NOTA-MMR Nb	Nanobody	Preclinical	–	(246)
	[^{68}Ga]Ga-NOTA-anti-MMR-VHH2	Nanobody	Clinical	NCT04168528 NCT04758650	–
FRβ	[^{18}F]α/γ-FBA-Folate	Folate derivative	Preclinical	–	(247)
	[^{18}F]click-folate	Folate derivative	Preclinical	–	(248)
	[^{68}Ga]DOTA-folate	Folate derivative	Preclinical	–	(249)
	2'-[^{18}F]fluorofolic acid	Folate derivative	Preclinical	–	(250)
	[^{18}F]fluorobenzene-folate	Folate derivative	Preclinical	–	(251)
	[^{18}F]pyridinecarbohydrazide-folate	Folate derivative	Preclinical	–	(251)
	[^{18}F]fluorodeoxy-glucose-folate	Folate derivative	Preclinical	–	(252–254)
	[^{68}Ga]NODAGA-folate	Folate derivative	Preclinical	–	(255)
	[^{68}Ga]DO3A-EA-Pte	Pteroic acid derivative	Preclinical	–	(256)
	3′-aza-2′[^{18}F]fluorofolicacid/[^{18}F]AzaFol	Folate derivative	Clinical	–	(257–259)
	[^{18}F]fluoro-PEG-folate	Folate derivative	Clinical	NCT05215496	(260–263)
	4-[^{18}F]-fluorophenylfolate	Folate derivative	Preclinical	–	(264)
	[^{68}Ga]NOTA-folate	Folate derivative	Preclinical	–	(265, 266)
	α/β-click[^{18}F]FDG-folate	Folate derivative	Preclinical	–	(267)
	α/β-click[^{18}F]FE-folate	Folate derivative	Preclinical	–	(267)

(Continued)

TABLE 2 | Continued

Target marker/ pathway	Radiotracer	Class	Clinical/ preclinical	Active clinical trials	References
	α/β-click[^{18}F]FB-folate	Folate derivative	Preclinical	–	(267)
	Folate-NOTA-Al[^{18}F]	Folate derivative	Preclinical	–	(268)
	[^{64}Cu]rf42	Folate derivative	Preclinical	–	(269)
	[^{68}Ga]rf42	Folate derivative	Preclinical	–	(269)
	[^{68}Ga]DOTA-Lys-Pteroyl	Pteroyl-Lys derivatives	Preclinical	–	(270)
	[^{68}Ga]DOTA-DAV-Lys-Pteroyl	Pteroyl-Lys derivatives	Preclinical	–	(270)
	[^{68}Ga]NOTA-folic acid	Folate derivative	Preclinical	–	(271)
	[^{89}Zr]FA-DFO-liposome	Folate coated liposome	Preclinical	–	(272)
	[^{68}Ga]HCEF	Folate derivative	Preclinical	–	(273)
	Folate-PEG12-NOTA-Al[^{18}F]	Folate derivative	Preclinical	–	(274)
	[^{64}Cu]DOTA-FA-FI-G5·NHAc dendrimers	Folate tagged dendrimers	Preclinical	–	(275)
	[^{18}F]Ala-folate	Folate derivative	Preclinical	–	(276)
	[^{18}F]DBCO-folate	Folate derivative	Preclinical	–	(276)
	[^{18}F]FOL	Folate derivative	Preclinical	–	(277, 278)
	[^{68}Ga]NODAGA-FA	Folate modified polymer	Preclinical	–	(279)
	[^{55}Co]Co-cm10	Folate derivative	Preclinical	–	(280)
	[^{55}Co]Co-rf42	Folate derivative	Preclinical	–	(280)
	[^{68}Ga]Ga-FA-I	Folate derivative	Preclinical	–	(281)
	[^{68}Ga]Ga-FA-II	Folate derivative	Preclinical	–	(281)
	[^{89}Zr]SFT-1	Folate coated nanoparticle	Preclinical	–	(282)
	[^{68}Ga]FOL	Folate derivative	Preclinical	–	(283)
	[^{89}Zr]FA-SMWs	Folate coated micro-silica	Preclinical	–	(284)
CD80/86	[^{64}Cu]NODAGA-abatacept	Biologic	Preclinical	–	(285)
iNOS	S-[^{11}C]methylisothiourea	iNOS inhibitor	Preclinical	–	(286)
	S-(2-[^{18}F]fluoroethyl)-isothiourea	iNOS inhibitor	Preclinical	–	(286)
	[^{18}F]FFDI	iNOS inhibitor	Preclinical	–	(287)
	[^{18}F]6-(2-fluoropropyl)-4-methyl-pyridin-2-amine	iNOS inhibitor	Preclinical	–	(288)
	[^{18}F]NOS	iNOS inhibitor	Clinical	NCT04062526	(289, 290)
	[^{18}F]FBAT	iNOS inhibitor	Preclinical	–	(291)
CCR2	[^{64}Cu]DOTA-ECL1i	Peptide	Clinical	NCT04217057 NCT03492762 NCT05107596 NCT04592991 NCT04537403 NCT03851237 NCT04586452	(292–300)
	[^{64}Cu]AuNCs-ECL1i	Peptide	Preclinical	–	(293)
	[^{64}Cu]Cu@CuO$_x$	Nanoparticle	Preclinical	–	(301)
	[^{18}F]6b	Chemical compound	Preclinical	–	(302)
CX3CR1	[^{11}C]methyl(2-amino-5(benzylthio)thiazolo[4,5-d]pyrimidin-7-yl)-d-leucinate	Chemical compound	Preclinical	–	(303)
VEGF	[^{124}I]HuMV833	Antibody	Clinical	–	(304)
	[^{124}I]iodinated-VG76e	Antibody	Preclinical	–	(305)
	[^{89}Zr]bevacizumab	Antibody	Clinical	–	(306–317)
	[^{64}Cu]DOTA-bevacizumab	Antibody	Preclinical	–	(318)
	[^{89}Zr]ranibizumab	Antibody	Preclinical	–	(319)
	[^{64}Cu] NOTA-Bev-800CW	Antibody	Preclinical	–	(320)
	[^{124}I]aflibercept	VEGF antagonist	Preclinical	–	(321)
	[^{64}Cu]NOTA-bevacizumab	Antibody	Preclinical	–	(322)
	[^{64}Cu]L19K-FDNB	Peptide	Preclinical	–	(323)

Inducible nitric oxide synthase (iNOS) is a reactive oxygen and nitrogen metabolite-metabolizing enzyme typically expressed by activated proinflammatory macrophages. The utility of [^{18}F]NOS, iNOS targeted radiotracer based on iNOS inhibitor has been reported in allograft rejection patients and patients with acute lung inflammation (289, 290). The studies also showed low brain radioactivity suitable for the imaging of C-GCA. Intimal infiltrating iNOS+ macrophages have been previously reported in GCA whereas in the adventitia of these vessels iNOS+ macrophages were absent (48). Therefore, iNOS imaging may be valuable as a tool to detect intimal macrophage infiltration and potentially intimal hyperplasia.

The chemokine receptors CCR2 and CX3CR1 are responsible for the trafficking of monocytes into the GCA affected vessel wall where these cells will then mature into macrophages (33). The radiotracer [^{64}Cu]DOTA-ECL1i specifically targeting CCR2 may be useful for imaging infiltrating monocytes/macrophages in GCA affected vessels. The utility of this radiotracer has recently been investigated in patients with pulmonary fibrosis (298). The study showed specific uptake in diseased lungs with little uptake in healthy controls. Moreover, low non-specific brain uptake and low blood radioactivity may be beneficial for imaging both LV-GCA and C-GCA. On the other hand, the radiotracer [^{11}C]methyl(2-amino-5-(benzylthio)thiazolo[4,5-d]pyrimidin-7-yl)-d-leucinate designed to target CX3CR1, failed to show specific binding to CX3CR1 and therefore is not suitable for imaging GCA at the current state (303). As CX3CR1+ monocyte infiltration was reported to be higher than CCR2+ monocytes, future radiotracers targeting CX3CR1 may be beneficial for the imaging of GCA.

The abundance of vascular endothelial growth factor (VEGF), a potent pro-angiogenic growth factor, has been reported in the synovium of PMR patients (55). Macrophages have been implicated as the major source of VEGF as these cells are the major cellular infiltrates in the inflamed synovium (55). The antibody-based radiotracer [^{89}Zr]bevacizumab targeting VEGF has been successfully used to visualize VEGF expression in multiple oncological conditions (308, 314–317). Additionally, the utility of [^{89}Zr]bevacizumab in detecting VEGF expression in atherosclerotic plaques has been shown in *ex vivo* imaging studies of human carotid endarterectomy (CEA) specimens (309). Since the increased expression of VEGF has been reported in PMR, [^{89}Zr]bevacizumab imaging may be useful for imaging PMR patients. Of note, although inflammatory macrophages are major producers of VEGF in PMR, infiltrating T cells are also capable of producing VEGF (55). Hence, VEGF-targeted imaging may not be specific for macrophages. In GCA, heightened VEGF expression has been documented especially in the adventitia of GCA-affected vessels (337). However, whether macrophages or T cells are the main producers of VEGF in GCA lesions remains to be further explored. Nevertheless, VEGF imaging may potentially also be useful for imaging GCA.

Most of the macrophage-targeted radiotracers discussed above may be suitable for imaging GCA. However, whether similar macrophage phenotypes are involved in the pathogenesis of PMR remains to be proven since, to our knowledge, no study to date has explored macrophage heterogeneity in PMR.

B Cell-Targeted Radiotracers

B cell infiltration and organization into TLOs have been well-documented in GCA (38, 338). However, B cell appear to be absent in the synovial tissue of PMR patients (54). Therefore, B cell-targeted imaging may only be suitable for GCA. Several B cells targeted radiotracers have been developed (**Table 3**).

A case report has documented the resolution of vascular inflammation in a GCA patient with rituximab B cell depletion therapy (354). However, no further trials are currently ongoing for rituximab therapy in GCA. Rituximab-based radiotracer [^{89}Zr]rituximab has been successfully used to image B cells in lymphoma and RA patients (347, 348). The radiotracer showed low background activity in the blood pool which may support its suitability for application in imaging GCA.

Activated Fibroblast Targeted Radiotracers

Remodeling of the arterial wall secondary to inflammation may cause vessel occlusion and hence, be responsible for the ischemic events in GCA. Fibroblast activation, migration, and proliferation in the intima have been reported as one of the causes of intimal hyperplasia (50). Currently, the targeted imaging of fibroblast activation protein alpha (FAP), a serine protease expressed mainly by activated fibroblast, is gaining tremendous interest in cancer and inflammatory diseases (355). The interest in FAP targeted imaging started with the development of radiolabeled FAP inhibitor [^{125}I]MIP-1232 for single-photon emission computed tomography (SPECT) imaging of atherosclerosis (356). However, *ex vivo,* the radiotracer showed uptake in normal arteries as well hampering its utility for atherosclerotic imaging. Since then, more specific FAP inhibitors (FAPIs) have been rapidly developed and radiolabeled as PET radiotracers (**Table 4**).

From these FAPI based radiotracers, [^{68}Ga]FAPI-04 has been rapidly implemented in clinical trials and has shown superiority compared to the long-time gold standard [^{18}F]FDG for imaging cancer and inflammation as recently summarized by Li et al. (355). These reports showed high and specific uptake in tumors as well as at sites of fibrosis and inflammation while displaying negligible blood pool and brain radioactivity supporting its potential application for imaging both C-GCA and LV-GCA. Although FAP expression has not yet been investigated in the context of GCA and PMR, a case report has shown successful visualization of aortic and arterial inflammation in a patient suffering from GCA using [^{68}Ga]FAPI-04 (368). Interestingly [^{68}Ga]FAPI-04 imaging showed negligible radioactivity in non-target organs including the brain, background tissue, and in the blood pool, which may allow accurate detection of C-GCA. This case report demonstrates the potential of FAP targeted imaging for visualization of vascular inflammation in GCA warranting further investigation especially in comparison with the current gold standard [^{18}F]FDG-PET. No reports have shown the utility of FAP targeted imaging in PMR patients to date. Yet, successful FAP targeted imaging has been demonstrated in RA patients which may point to its potential to image inflammation in PMR patients as well (369).

TABLE 3 | B cell targeted PET radiotracers.

Target marker/ pathway	Radiotracer	Class	Clinical/ preclinical	Active clinical trials	References
CD20	[64Cu]DOTA-minibody (based on rituximab)	Minibody	Preclinical	–	(339)
	[124I]anti-CD20-Cys-Db (based on rituximab)	Diabody	Preclinical	–	(340)
	[124I]rituximab	Antibody	Clinical	–	(341, 342)
	[89Zr]rituximab	Antibody	Clinical	–	(343–348)
	[64Cu]DOTA-rituximab	Antibody	Preclinical	–	(349, 350)
	[64Cu]FN3(CD20)	Protein	Preclinical	–	(351)
	[18F]FB-GAcDb (based on obinutuzumab)	Diabody	Preclinical	–	(352)
	[89Zr]GacDb (based on obinutuzumab)	Diabody	Preclinical	–	(353)
	[89Zr]GacMb (based on obinutuzumab)	Minibody	Preclinical	–	(353)

TABLE 4 | Fibroblast activation protein alpha (FAP) targeted PET radiotracers.

Radiotracer	Class	Clinical/preclinical	Active clinical trials	References
[68Ga]FAPI-02	FAP inhibitor	Preclinical	–	(357)
[68Ga]DOTA.SA.FAPI	FAP inhibitor	Clinical	–	(358, 359)
[68Ga]FAPI-04/[68Ga]DOTA-FAPI-04	FAP inhibitor	Clinical	NCT05003427 NCT04504110 NCT04533828 NCT04441606 NCT04499365 NCT04831034 NCT04416165 NCT05121779 NCT05140746	(357)
[68Ga]NOTA-FAPI-04	FAP inhibitor	Clinical	NCT04499365 NCT04367948 NCT04750772 NCT05004961	(360)
[68Ga]FAPI-21	FAP inhibitor	Clinical	–	(361)
[68Ga]FAPI-46	FAP inhibitor	Clinical	NCT05160051 NCT04941872 NCT04457258 NCT04457232 NCT04459273 NCT04147494 NCT05172310	(361)
[68Ga]TEFAPI-06	FAP inhibitor	Preclinical	–	(362)
[68Ga]TEFAPI-07	FAP inhibitor	Preclinical	–	(362)
[68Ga]FAPI-C12	FAP inhibitor	Preclinical	–	(363)
[68Ga]FAPI-C16	FAP inhibitor	Preclinical	–	(363)
[68Ga]FAPtp	FAP inhibitor	Preclinical	–	(364)
[68Ga]Aib-FAPtp-01	FAP inhibitor	Preclinical	–	(364)
[68Ga]DOTA-2P(FAPI)$_2$	FAP inhibitor	Clinical	NCT04941872	(365)
[18F]FGlc-FAPI	FAP inhibitor	Preclinical	–	(366)
Al[18F]NOTA-FAPI	FAP inhibitor	Clinical		(367)
[18F]NOTA-FAPI-04	FAP inhibitor	Clinical	NCT04367948 NCT04750772 NCT05004961	–

Endothelial Cell-Targeted Radiotracers

Neoangiogenesis is one of the crucial pathogenic features of GCA and PMR. Increased vascularity in the vessel wall and synovium of GCA and PMR patients further enables the invasion of leukocytes thereby fueling the inflammatory process (32, 54, 55). In uninflamed vessels, the luminal endothelium does not express the inducible adhesion molecules VCAM-1. In inflamed GCA-affected vessels, the intense expression of VCAM-1 has been

reported on neovessel endothelial cells making this adhesion molecule suitable for targeted imaging (32). Several radiotracers targeting VCAM-1 have been developed (**Table 5**) which may be useful for imaging GCA.

An alternative approach to image angiogenesis is to target the integrin αvβ3 and specific radiotracers for this integrin have already been applied in clinical practice for imaging tumor metastasis (374–376). However, whether this approach is suitable for imaging GCA is uncertain since the αvβ3 integrin is constitutively expressed on the luminal endothelium (377). Nevertheless, studies have demonstrated the enhanced uptake of αvβ3 integrin-targeted tracers in atherosclerotic plaques corresponding to neo-vessel formation indicating its potential utility in GCA (374, 378). Furthermore, imaging integrin αvβ3 may be of interest for PMR as increased vascularization has been reported in the synovial tissues from PMR patients. Of note, integrin αvβ3 imaging is not specific for angiogenesis as infiltrating leukocytes can also express this adhesion molecule (379).

FUTURE PERSPECTIVES: TOWARD DISEASE STRATIFICATION AND BETTER TREATMENT MONITORING

The molecular PET imaging technique targeting specific markers has made valuable contributions to clinical practice ranging from diagnosis, staging, and prognosis to treatment monitoring. There are clear examples in other fields of medicine, mainly from the field of oncology, supporting the use of targeted imaging in patient stratification for targeted therapy. For example, anti-human epidermal growth factor receptor 2 (HER2) targeted therapy is only effective in HER2+ breast cancer accounting for only up to 30% of newly diagnosed breast cancer patient which can be visualized by HER2 targeted PET imaging (380–383). In another study, HER2+ PET imaging using [^{89}Zr]trastuzumab in combination with [^{18}F]FDG resulted in a negative and positive predictive value of 100% for discriminating between patients with a time to treatment failure of 2.8 and 15 months (384). A recent preclinical study in a cancer mouse model, *in vivo* imaging of different receptor tyrosine kinases (RTKs) demonstrated a decrease in receptor expression levels after their respective targeted therapy (385). Beyond oncology, [^{18}F]FDOPA PET imaging of striatal dopaminergic system has been shown to effectively stratify responders and non-responders of antipsychotic treatment in schizophrenic patients (386). Collectively, these studies support the utility of targeted PET imaging in aiding patient stratification for specific treatment strategies, prognosis and precision monitoring of treatment effect in inflammatory diseases including GCA and PMR.

In imaging GCA and PMR, radiotracers targeting specific cell populations may potentially be superior compared to the current gold standard [^{18}F]FDG. The majority of the novel PET radiotracers listed above have shown low non-target organ uptake, especially in the brain, which could increase the TBR and may translate into improved detection of cranial artery inflammation in patients suffering from C-GCA. Additionally,

several novel radiotracers show low blood pool radioactivity assuring optimal TBR and visualization of aortic and arterial inflammation in LV-GCA.

Since persistent T cell and macrophage infiltration has been reported in TAB of patients undergoing glucocorticoid treatment (59, 60), imaging T cell and macrophage subsets could, in theory, be superior to [^{18}F]FDG in the diagnostic imaging of GCA. Similarly, these radiotracers could also be useful for the diagnostic imaging of PMR as persistent T cell and macrophage infiltration has also been shown in PMR patients undergoing GC treatment (54).

Imaging specific leukocyte populations may have prognostic value and may help in designing personalized treatment regimens for GCA and PMR (387). The utility of immune cell targeted imaging has indeed been reported in the context of oncology and in autoimmune inflammatory diseases. An example of this was reported in a study conducted using [^{99m}TC]IL-2 scintigraphy in melanoma patients. The study showed successful visualization of tumor infiltrating lymphocytes which enables the selection of patient whom may benefit from IL-2 immunotherapy (388). Another example was reported in patients with rheumatoid arthritis (RA) using B cell targeted [^{89}Zr]rituximab (348). The study showed that patients who responded to B cells depletion therapy had higher baseline imaging signal. In the context of GCA, the higher intensity of CD8+ T cell infiltration in the vessel wall of GCA patients has been proposed as a risk factor for visual impairment and a longer GC treatment dependency. This suggests that CD8+ T cell imaging in GCA may confer prognostic value (35). In the B cell compartment, CD20-based imaging could prove to be useful as a theranostic approach to identify GCA patients that may benefit from rituximab treatment followed by a therapeutic dose of rituximab after imaging confirmation (354). In another example, we have previously reported the prognostic value of serum levels of YKL-40 in patients suffering from GCA (389). Higher levels of serum YKL-40 at baseline predicted a longer duration of GC treatment. In the GCA-affected vessel wall, YKL-40 is highly expressed by GM-CSF skewed CD206+ macrophages (42). Therefore, imaging the extent of CD206+ infiltration in the vessels may also predict the GC dependency of these patients. Recently, a phase II clinical trial with a GM-CSF receptor blocker (mavrilimumab) demonstrated GM-CSF receptor blockade to be efficacious in the treatment of GCA (390). Furthermore, *ex vivo* treatment of GCA-affected vessels with mavrilimumab documented a reduction of CD206 expression (40). Based on these studies, imaging CD206 in GCA patients may potentially identify patients that could benefit from mavrilimumab treatment. Along similar lines, the cytokine IL-6 has been reported to elevate the expression of CD163 on macrophages (5). Hence, the detection of CD163+ macrophages may reveal GCA patients that could benefit from the IL-6 receptor blocker, tocilizumab. Although no report has shown infiltration of CD163+ macrophages in PMR, IL-6 is a major cytokine involved in the pathogenesis of this disease denoting the possibility of CD163+ macrophage infiltration in the synovium of PMR patients. Unfortunately, the only CD163 targeted radiotracer currently reported was developed for preclinical imaging in rat models but does not cross-react with

TABLE 5 | Adhesion molecule VCAM-1 targeted PET radiotracers.

Target marker/ pathway	Radiotracer	Class	Clinical/ preclinical	Active clinical trials	References
VCAM-1	[^{18}F]4V	Peptide	Preclinical	–	(370)
	[^{18}F]-FB-anti-VCAM-1 Nb	Nanobody	Preclinical	–	(371)
	[^{68}Ga]NOTA-VCAM-1$_{scFv}$	Antibody fragment	Preclinical	–	(372)
	[^{68}Ga]MacroP	Peptide	Preclinical	–	(373)
	NAMP–avidin–[^{68}Ga]–BisDOTA	Peptide	Preclinical	–	(373)

human CD163 (391). Future development of CD163 targeted tracers may be beneficial for the imaging of GCA patients and potentially PMR patients.

The novel radiotracers discussed in this review may also be used for monitoring treatment efficacy. Reduced numbers of T cells and macrophages at the site of inflammation have been reported (54, 59, 60). This may translate to a gradual decrease in imaging signal during treatment which could be useful for monitoring ongoing inflammation during GC treatment. Furthermore, the reduced expression of endothelial adhesion molecules VCAM-1 and E-selectin has been reported in the vessels of GCA patients undergoing GC treatment (32). In addition, targeted imaging of specific cell populations could also be used for monitoring the efficacy of novel immunotherapies. Reduced CD206 expression and neovascularization have been reported in *ex vivo* cultured temporal artery explants of GCA patients treated with mavrilimumab (40). Therefore, tracking the dynamics of these cellular markers by imaging may be useful for treatment effect monitoring in patients undergoing mavrilimumab treatment.

Although these novel radiotracers may be useful for imaging GCA and PMR, several considerations have to be taken into account before these tracers can be applied in clinical practice. Firstly, some of these novel tracers are tagged with radionuclides with high radiation doses such as ^{89}Zr (392). Nuclides with high radioactivity are necessary for tracers based on large molecules with low tissue penetration rates such as antibodies. The long half-life of ^{89}Zr (3.3 days) allows a longer period of time for effective tissue penetration and blood clearance to ensure that the signal can be imaged after a prolonged time frame after injection. This higher radiation dose is permissible in imaging oncology patients but is not recommended for patients with autoimmune and inflammatory diseases such as GCA and PMR. Therefore, it is important to develop radiotracers with better tissue penetration rates and tagged with radionuclides with lower radiation burdens such as ^{18}F. The current emerging technology employing camelid-based nanobody is promising in this regard (393). Secondly, these novel radiotracers are not readily available due to the production complexity and cost compared to [^{18}F]FDG (394, 395). Future research into an improved methodology for the economical and rapid production of these novel tracers is imperative to bring these into clinical practice. Finally, although theoretically the novel radiotracers mentioned in this review may be useful for the imaging of GCA and PMR, clinical trials are needed to evaluate and confirm their utility in the diagnosis and monitoring of GCA and PMR.

SUMMARY AND CONCLUSION

Due to progress in our understanding of the immunopathology of GCA/PMR and the development of novel, highly specific tracers, direct imaging of immune cells/mediators by PET is now within reach. Such novel PET imaging strategies targeting a specific subset of inflammatory cells and activation markers of resident cells could be valuable diagnostic tools in GCA/PMR. Furthermore, direct imaging of infiltrating immune cells and inflammatory mediators might be useful for the treatment monitoring of GCA and PMR patients. Eventually, these novel radiotracers may also hold promise for disease stratification in GCA/PMR, since these tracers could help to select patients that may benefit from particular treatment regimens. The majority of these novel radiotracers are still mainly used as research tools in academic centers. Efforts are needed to evaluate these radiotracers in larger clinical trials to validate their utility in clinical practice. The introduction and implementation of such novel tracers will require close collaboration between patients, clinicians (e.g., rheumatologists, internists), nuclear medicine specialists and immunologists.

AUTHOR CONTRIBUTIONS

KG: conceptualization, conducted a review of the literature, and writing—review and editing. MS, PN, RS, and PH: writing—review and editing. EB: conceptualization and writing—review and editing. WJ: conceptualization, conducted a review of the literature, writing—original draft preparation, and writing—review and editing. All authors provide approval for publication of the content and agreed to be accountable for all aspects of the work.

FUNDING

REFERENCES

1. Li KJ, Semenov D, Turk M, Pope J, A. meta-analysis of the epidemiology of giant cell arteritis across time and space. *Arthritis Res Ther.* (2021) 23:1–10. doi: 10.1186/s13075-021-02450-w

2. Robinette ML, Rao DA, Monach PA. The immunopathology of giant cell arteritis across disease spectra. *Front Immunol.* (2021) 12:623716. doi: 10.3389/fimmu.2021.623716

3. Dejaco C, Brouwer E, Mason JC, Buttgereit F, Matteson EL, Dasgupta B. Giant cell arteritis and polymyalgia rheumatica: current challenges and opportunities. *Nat Rev Rheumatol.* (2017) 13:578–92. doi: 10.1038/nrrheum.2017.142

4. Van Der Geest KSM, Sandovici M, Brouwer E, Mackie SL. Diagnostic accuracy of symptoms, physical signs, and laboratory tests for giant cell arteritis: a systematic review and meta-analysis. *JAMA Intern Med.* (2020) 180:1295–304. doi: 10.1001/jamainternmed.2020.3050

5. Esen I, Jiemy WF, van Sleen Y, van der Geest KSM, Sandovici M, Heeringa P, et al. Functionally heterogenous macrophage subsets in the pathogenesis of giant cell arteritis: novel targets for disease monitoring and treatment. *J Clin Med.* (2021) 10:4958. doi: 10.3390/jcm10214958

6. Hysa E, Gotelli E, Sammorì S, Cimmino MA, Paolino S, Pizzorni C, et al. Immune system activation in polymyalgia rheumatica: which balance between autoinflammation and autoimmunity? A systematic review. *Autoimmun Rev.* (2022) 21:102995. doi: 10.1016/j.autrev.2021.102995

7. Sharma A, Mohammad A, Turesson C. Incidence and prevalence of giant cell arteritis and polymyalgia rheumatica: a systematic literature review. *Semin Arthritis Rheum.* (2020) 50:1040–8. doi: 10.1016/j.semarthrit.2020.07.005

8. Sandovici M, van der Geest N, van Sleen Y, Brouwer E. Need and value of targeted immunosuppressive therapy in giant cell arteritis. *RMD Open.* (2022) 8:e001652. doi: 10.1136/rmdopen-2021-001652

9. Pujades-Rodriguez M, Morgan AW, Cubbon RM, Wu J. Dose-dependent oral glucocorticoid cardiovascular risks in people with immune-mediated inflammatory diseases: a population-based cohort study. *PLoS Med.* (2020) 17: 3432. doi: 10.1371/journal.pmed.1003432

10. Stone JH, Tuckwell K, Dimonaco S, Klearman M, Aringer M, Blockmans D, et al. Trial of tocilizumab in giant-cell arteritis. *N Engl J Med.* (2017) 377:317–28. doi: 10.1056/NEJMoa1613849

11. Devauchelle-Pensec V, Berthelot JM, Cornec D, Renaudineau Y, Marhadour T, Jousse-Joulin S, et al. Efficacy of first-line tocilizumab therapy in early polymyalgia rheumatica: a prospective longitudinal study. *Ann Rheum Dis.* (2016) 75:1506–10. doi: 10.1136/annrheumdis-2015-208742

12. Bonelli M, Radner H, Kerschbaumer A, Mrak D, Durechova M, Stieger J, et al. Tocilizumab in patients with new onset polymyalgia rheumatica (PMR-SPARE): a phase 2/3 randomised controlled trial. *Ann Rheum Dis.* (2022) 81:838–44. doi: 10.1136/annrheumdis-2021-221126

13. Hunder GG, Bloch DA, Michel BA, Stevens MB, Arend WP, Calabrese LH, et al. The American College of Rheumatology 1990 criteria for the classification of giant cell arteritis. *Arthritis Rheum.* (2010) 33:1122–8. doi: 10.1002/art.1780330810

14. Mahmood S. Bin, Nelson E, Padniewski J, Nasr R. Polymyalgia rheumatica: an updated review. *Cleve Clin J Med.* (2020) 87:549–56. doi: 10.3949/ccjm.87a.20008

15. Aschwanden M, Schegk E, Imfeld S, Staub D, Rottenburger C, Berger CT, et al. Vessel wall plasticity in large vessel giant cell arteritis: an ultrasound follow-up study. *Rheumatology.* (2019) 58:792–7. doi: 10.1093/rheumatology/key383

16. van der Geest KSM, Treglia G, Glaudemans AWJM, Brouwer E, Sandovici M, Jamar F, et al. Diagnostic value of [18F]FDG-PET/CT for treatment monitoring in large vessel vasculitis: a systematic review and meta-analysis. *Eur J Nucl Med Mol Imaging.* (2021) 48:3886–902. doi: 10.1007/s00259-021-05362-8

17. van der Geest KSM, Treglia G, Glaudemans AWJM, Brouwer E, Jamar F, Slart RHJA, et al. Diagnostic value of [18F]FDG-PET/CT in polymyalgia rheumatica: a systematic review and meta-analysis. *Eur J Nucl Med Mol Imaging.* (2021) 48:1876–89. doi: 10.1007/s00259-020-05162-6

18. Hellmich B, Agueda A, Monti S, Buttgereit F, De Boysson H, Brouwer E, et al. 2018 Update of the EULAR recommendations for the

19. Nienhuis PH, Sandovici M, Glaudemans AW, Slart RH, Brouwer E. Visual and semiquantitative assessment of cranial artery inflammation with FDG-PET/CT in giant cell arteritis. *Semin Arthritis Rheum.* (2020) 50:616–23. doi: 10.1016/j.semarthrit.2020.04.002

20. Nielsen BD, Hansen IT, Kramer S, Haraldsen A, Hjorthaug K, Bogsrud TV, et al. Simple dichotomous assessment of cranial artery inflammation by conventional 18F-FDG PET/CT shows high accuracy for the diagnosis of giant cell arteritis: a case-control study. *Eur J Nucl Med Mol Imaging.* (2019) 46:184–93. doi: 10.1007/s00259-018-4106-0

21. Pijl JP, Nienhuis PH, Kwee TC, Glaudemans AWJM, Slart RHJA, Gormsen LC. Limitations and pitfalls of FDG-PET/CT in infection and inflammation. *Semin Nucl Med.* (2021) 51:633–45. doi: 10.1053/j.semnuclmed.2021.06.008

22. Nielsen BD, Gormsen LC, Hansen IT, Keller KK, Therkildsen P, Hauge EM. Three days of high-dose glucocorticoid treatment attenuates large-vessel 18F-FDG uptake in large-vessel giant cell arteritis but with a limited impact on diagnostic accuracy. *Eur J Nucl Med Mol Imaging.* (2018) 45:1119–28. doi: 10.1007/s00259-018-4021-4

23. Lu Y, Liu H, Bi Y, Yang H, Li Y, Wang J, et al. Glucocorticoid receptor promotes the function of myeloid-derived suppressor cells by suppressing HIF1α-dependent glycolysis. *Cell Mol Immunol.* (2018) 15:618–29. doi: 10.1038/cmi.2017.5

24. Buentke E, Nordström A, Lin H, Björklund AC, Laane E, Harada M, et al. Glucocorticoid-induced cell death is mediated through reduced glucose metabolism in lymphoid leukemia cells. *Blood Cancer J.* (2011) 1:e31. doi: 10.1038/bcj.2011.27

25. Krupa WM, Dewan M, Jeon MS, Kurtin PJ, Younge BR, Goronzy JJ, et al. Trapping of misdirected dendritic cells in the granulomatous lesions of giant cell arteritis. *Am J Pathol.* (2002) 161:1815–23. doi: 10.1016/S0002-9440(10)64458-6

26. Weyand CM, Tetzlaff N, Björnsson J, Brack A, Younge B, Goronzy JJ. Disease patterns and tissue cytokine profiles in giant cell arteritis. *Arthritis Rheum.* (1997) 40:19–26. doi: 10.1002/art.1780400105

27. Conway R, O'Neill L, McCarthy GM, Murphy CC, Fabre A, Kennedy S, et al. Interleukin 12 and interleukin 23 play key pathogenic roles in inflammatory and proliferative pathways in giant cell arteritis. *Ann Rheum Dis.* (2018) 77:1815–24. doi: 10.1136/annrheumdis-2018-213488

28. Espígol-Frigolé G, Corbera-Bellalta M, Planas-Rigol E, Lozano E, Segarra M, García-Martínez A, et al. Increased IL-17A expression in temporal artery lesions is a predictor of sustained response to glucocorticoid treatment in patients with giant-cell arteritis. *Ann Rheum Dis.* (2013) 72:1481–7. doi: 10.1136/annrheumdis-2012-201836

29. Ciccia F, Rizzo A, Guggino G, Cavazza A, Alessandro R, Maugeri R, et al. Difference in the expression of IL-9 and IL-17 correlates with different histological pattern of vascular wall injury in giant cell arteritis. *Rheumatology.* (2015) 54:1596–604. doi: 10.1093/rheumatology/kev102

30. Cadena RH, Reitsema RD, Huitema MG, van Sleen Y, van der Geest KSM, Heeringa P, et al. Decreased expression of negative immune checkpoint VistA by CD4+ T cells facilitates T helper 1, T helper 17, and T follicular helper lineage differentiation in GCA. *Front Immunol.* (2019) 10:1638. doi: 10.3389/fimmu.2019.01638

31. Zhang H, Watanabe R, Berry GJ, Vaglio A, Liao YJ, Warrington KJ, et al. Immunoinhibitory checkpoint deficiency in medium and large vessel vasculitis. *Proc Natl Acad Sci USA.* (2017) 114:E970–9. doi: 10.1073/pnas.1616848114

32. Cid MC, Cebrián M, Font C, Coll-Vinent B, Hernández-Rodríguez J, Esparza J, et al. Cell adhesion molecules in the development of inflammatory infiltrates in giant cell arteritis: inflammation-induced angiogenesis as the preferential site of leukocyte-endothelial cell interactions. *Arthritis Rheum.* (2000) 43:184–94. doi: 10.1002/1529-0131(200001)43:1<184::AID-ANR23>3.0.CO;2-N

33. van Sleen Y, Wang Q, van der Geest KSM, Westra J, Abdulahad WH, Heeringa P, et al. Involvement of monocyte subsets in the immunopathology of giant cell arteritis. *Sci Rep.* (2017) 7:6553. doi: 10.1038/s41598-017-06826-4

34. Corbera-Bellalta M, Planas-Rigol E, Lozano E, Terrades-García N, Alba MA, Prieto-González S, et al. Blocking interferon γ reduces expression

of chemokines CXCL9, CXCL10 and CXCL11 and decreases macrophage infiltration in *ex vivo* cultured arteries from patients with giant cell arteritis. *Ann Rheum Dis.* (2016) 75:1177–86. doi: 10.1136/annrheumdis-2015-208371

35. Samson M, Ly KH, Tournier B, Janikashvili N, Trad M, Ciudad M, et al. Involvement and prognosis value of CD8(+) T cells in giant cell arteritis. *J Autoimmun.* (2016) 72:73–83. doi: 10.1016/j.jaut.2016.05.008

36. Reitsema RD, Boots AMH, van der Geest KSM, Sandovici M, Heeringa P, Brouwer E. CD8+ T cells in GCA and GPA: bystanders or active contributors? *Front Immunol.* (2021) 12:654109. doi: 10.3389/fimmu.2021.654109

37. Graver JC, Abdulahad W, van der Geest KSM, Heeringa P, Boots AMH, Brouwer E, et al. Association of the CXCL9-CXCR3 and CXCL13-CXCR5 axes with B-cell trafficking in giant cell arteritis and polymyalgia rheumatica. *J Autoimmun.* (2021) 123:102684. doi: 10.1016/j.jaut.2021.102684

38. Graver JC, Boots AMH, Haacke EA, Diepstra A, Brouwer E, Sandovici M. Massive B-cell infiltration and organization into artery tertiary lymphoid organs in the aorta of large vessel giant cell arteritis. *Front Immunol.* (2019) 10:83. doi: 10.3389/fimmu.2019.00083

39. Graver JC, Jiemy WF, Altulea D, Boots A, Heeringa P, Abdulahad W, Brouwer E, Sandovici M. OP0062 cytokine producing B cells skew macrophages towards a pro-inflammatory phenotype in giant cell arteritis. *Ann Rheum Dis.* (2021) 80:33.1–34. doi: 10.1136/annrheumdis-2021-eular.1984

40. Corbera-Bellalta M, Alba-Rovira R, Muralidharan S, Espígol-Frigolé G, Ríos-Garcés R, Marco-Hernández J, et al. Blocking GM-CSF receptor α with mavrilimumab reduces infiltrating cells, pro-inflammatory markers and neoangiogenesis in *ex vivo* cultured arteries from patients with giant cell arteritis. *Ann Rheum Dis.* (2022) 81:524–36. doi: 10.1136/annrheumdis-2021-220873

41. Jiemy WF, van Sleen Y, van der Geest KSM, ten Berge HA, Abdulahad WH, Sandovici M, et al. Distinct macrophage phenotypes skewed by local granulocyte macrophage colony-stimulating factor (GM-CSF) and macrophage colony-stimulating factor (M-CSF) are associated with tissue destruction and intimal hyperplasia in giant cell arteritis. *Clin Transl Immunol.* (2020) 9:e1164. doi: 10.1002/cti2.1164

42. van Sleen Y, Jiemy WF, Pringle S, van der Geest KSM, Abdulahad WH, Sandovici M, et al. Distinct macrophage subset mediating tissue destruction and neovascularization in giant cell arteritis: implication of the YKL-40/interleukin-13 receptor α2 axis. *Arthritis Rheumatol.* (2021) 73:2327–37. doi: 10.1002/art.41887

43. Esen I, Jiemy WF, van Sleen Y, Bijzet J, de Jong DM, Nienhuis PH, et al. Plasma Pyruvate kinase M2 as a marker of vascular inflammation in giant cell arteritis. *Rheumatology.* (2021). doi: 10.1093/rheumatology/keab814. [Epub ahead of print].

44. Johansen JS, Baslund B, Garbarsch C, Hansen M, Stoltenberg M, Lorenzen I, et al. YKL-40 in giant cells and macrophages from patients with giant cell arteritis. *Arthritis Rheum.* (1999) 42:2624–30. doi: 10.1002/1529-0131(199912)42:12<2624::AID-ANR17>3.0.CO;2-K

45. Watanabe R, Maeda T, Zhang H, Berry GJ, Zeisbrich M, Brockett R, et al. (matrix metalloprotease)-9-producing monocytes enable T cells to invade the vessel wall and cause vasculitis. *Circ Res.* (2018) 123:700–15. doi: 10.1161/CIRCRESAHA.118.313206

46. Rittner HL, Kaiser M, Brack A, Szweda LI, Goronzy JJ, Weyand CM. Tissue-destructive macrophages in giant cell arteritis. *Circ Res.* (1999) 84:1050–8. doi: 10.1161/01.RES.84.9.1050

47. Ciccia F, Alessandro R, Rizzo A, Raimondo S, Giardina AR, Raiata F, et al. IL-33 is overexpressed in the inflamed arteries of patients with giant cell arteritis. *Ann Rheum Dis.* (2013) 72:258–64. doi: 10.1136/annrheumdis-2012-201309

48. Weyand CM, Wagner AD, Björnsson J, Goronzy JJ. Correlation of the topographical arrangement and the functional pattern of tissue-infiltrating macrophages in giant cell arteritis. *J Clin Invest.* (1996) 98:1642–9. doi: 10.1172/JCI118959

49. Planas-Rigol E, Terrades-Garcia N, Corbera-Bellalta M, Lozano E, Alba MA, Segarra M, et al. Endothelin-1 promotes vascular smooth muscle cell migration across the artery wall: a mechanism contributing to vascular remodelling and intimal hyperplasia in giant-cell arteritis. *Ann Rheum Dis.* (2017) 76:1623–33. doi: 10.1136/annrheumdis-2016-210792

50. Parreau S, Vedrenne N, Regent A, Richard L, Sindou P, Mouthon L, et al. An immunohistochemical analysis of fibroblasts in giant cell arteritis. *Ann Diagn Pathol.* (2021) 52:151728. doi: 10.1016/j.anndiagpath.2021.151728

51. Akiyama M, Ohtsuki S, Berry GJ, Liang DH, Goronzy JJ, Weyand CM. Innate and adaptive immunity in giant cell arteritis. *Front Immunol.* (2020) 11:621098. doi: 10.3389/fimmu.2020.621098

52. Petursdottir V, Nordborg E, Nordborg C. Atrophy of the aortic media in giant cell arteritis. *APMIS.* (1996) 104:191–8. doi: 10.1111/j.1699-0463.1996.tb00707.x

53. Gordon I, Rennie AM, Branwood AW. Polymyalgia rheumatica: biopsy studies. *Ann Rheum Dis.* (1964) 23:447. doi: 10.1136/ard.23.6.447

54. Meliconi R, Pulsatelli L, Uguccioni M, Salvarani C, Macchioni P, Melchiorri C, et al. Leukocyte infiltration in synovial tissue from the shoulder of patients with polymyalgia rheumatica. Quantitative analysis and influence of corticosteroid treatment. *Arthritis Rheum.* (1996) 39:1199–207. doi: 10.1002/art.1780390719

55. Meliconi R, Pulsatelli L, Dolzani P, Boiardi L, Macchioni P, Salvarani C, et al. Vascular endothelial growth factor production in polymyalgia rheumatica. *Arthritis Rheum.* (2000) 43:2472–80. doi: 10.1002/1529-0131(200011)43:11<2472::AID-ANR14>3.0.CO;2-B

56. Reitsema R, Wekema L, Abdulahad W, Heeringa P, Huitema M, Sandovici M, et al. Characterization of synovial fluid T cells in polymyalgia rheumatica: implication of Th1 and Tc1 effector memory profiles [abstract]. *Arthrit Rheumatol.* (2021) 73:(suppl .10).

57. Zhu X, Lee CW, Xu H, Wang YF, Yung PSH, Jiang Y, et al. Phenotypic alteration of macrophages during osteoarthritis: a systematic review. *Arthritis Res Ther.* (2021) 23:1–13. doi: 10.1186/s13075-021-02457-3

58. Tardito S, Martinelli G, Soldano S, Paolino S, Pacini G, Patane M, et al. Macrophage M1/M2 polarization and rheumatoid arthritis: a systematic review. *Autoimmun Rev.* (2019) 18:102397. doi: 10.1016/j.autrev.2019.102397

59. Maleszewski JJ, Younge BR, Fritzlen JT, Hunder GG, Goronzy JJ, Warrington KJ, et al. Clinical and pathological evolution of giant cell arteritis: a prospective study of follow-up temporal artery biopsies in 40 treated patients. *Mod Pathol.* (2017) 30:788. doi: 10.1038/modpathol.2017.10

60. Jakobsson K, Jacobsson L, Mohammad AJ, Nilsson JÅ, Warrington K, Matteson EL, et al. The effect of clinical features and glucocorticoids on biopsy findings in giant cell arteritis. *BMC Musculoskelet Disord.* (2016) 17:363. doi: 10.1186/s12891-016-1225-2

61. Li HY, Xu JN, Shuai ZW. Cellular signaling pathways of T cells in giant cell arteritis. *J Geriatr Cardiol.* (2021) 18:768–78. doi: 10.11909/j.issn.1671-5411.2021.09.008

62. Di Gialleonardo V, Signore A, Willemsen ATM, Sijbesma JWA, Dierckx RAJO, De Vries EFJ. Pharmacokinetic modelling of N-(4-[(18)F]fluorobenzoyl)interleukin-2 binding to activated lymphocytes in an xenograft model of inflammation. *Eur J Nucl Med Mol Imaging.* (2012) 39:1551–60. doi: 10.1007/s00259-012-2176-y

63. van de Donk PP, Wind TT, Hooiveld-Noeken JS, van der Veen EL, Glaudemans AWJM, Diepstra A, et al. Interleukin-2 PET imaging in patients with metastatic melanoma before and during immune checkpoint inhibitor therapy. *Eur J Nucl Med Mol Imaging.* (2021) 48:4369–76. doi: 10.1007/s00259-021-05407-y

64. Di Gialleonardo V, Signore A, Glaudemans AWJM, Dierckx RAJO, De Vries EFJ. N-(4-18F-fluorobenzoyl)interleukin-2 for PET of human-activated T lymphocytes. *J Nucl Med.* (2012) 53:679–86. doi: 10.2967/jnumed.111.091306

65. Van der Veen EL, Suurs F V, Cleeren F, Bormans G, Elsinga PH, Hospers GAP, et al. Development and evaluation of interleukin-2–derived radiotracers for PET imaging of T cells in mice. *J Nucl Med.* (2020) 61:1355. doi: 10.2967/jnumed.119.238782

66. Traenkle B, Kaiser PD, Pezzana S, Richardson J, Gramlich M, Wagner TR, et al. Single-domain antibodies for targeting, detection, and *in vivo* imaging of human CD4+ cells. *Front Immunol.* (2021) 12:799910. doi: 10.3389/fimmu.2021.799910

67. Nagle VL, Hertz CAJ, Henry KE, Graham MS, Campos C, Pillarsetty N, et al.. Non-invasive imaging of CD4+ T cells in humanized mice. *Mol Cancer Ther.* (2022) 21:658–66. doi: 10.1158/1535-7163.MCT-21-0888

68. Maresca KP, Chen J, Mathur D, Giddabasappa A, Root A, Narula J, et al. Preclinical evaluation of 89 Zr-Df-IAB22M2C PET as an imaging biomarker for the development of the GUCY2C-CD3 bispecific PF-07062119 as a T cell engaging therapy. *Mol Imaging Biol.* (2021) 23:941–51. doi: 10.1007/s11307-021-01621-0

69. Griessinger CM, Olafsen T, Mascioni A, Jiang ZK, Zamilpa C, Jia F, et al. The PET-tracer 89 Zr-Df-IAB22M2C enables monitoring of intratumoral CD8 T-cell infiltrates in tumor-bearing humanized mice after T-cell bispecific antibody treatment. *Cancer Res.* (2020) 80:2903–13. doi: 10.1158/0008-5472.CAN-19-3269

70. Farwell MD, Gamache RF, Babazada H, Hellmann MD, Harding JJ, Korn R, et al. CD8-targeted PET imaging of tumor infiltrating T cells in patients with cancer: a phase I first-in-human study of 89 Zr-Df-IAB22M2C, a radiolabeled anti-CD8 minibody. *J Nucl Med.* (2021) 63:720–6. doi: 10.2967/jnumed.121.262485

71. Pandit-Taskar N, Postow MA, Hellmann MD, Harding JJ, Barker CA, O'Donoghue JA, et al. First-in-humans imaging with 89 Zr-Df-IAB22M2C anti-CD8 minibody in patients with solid malignancies: preliminary pharmacokinetics, biodistribution, and lesion targeting. *J Nucl Med.* (2020) 61:512–9. doi: 10.2967/jnumed.119.229781

72. Mitra S, Leonard WJ. Biology of IL-2 and its therapeutic modulation: mechanisms and strategies. *J Leukoc Biol.* (2018) 103:643–55. doi: 10.1002/JLB.2RI0717-278R

73. van der Geest KSM, Abdulahad WH, Teteloshvili N, Tete SM, Peters JH, Horst G, et al. Low-affinity TCR engagement drives IL-2-dependent post-thymic maintenance of naive CD4+ T cells in aged humans. *Aging Cell.* (2015) 14:744–53. doi: 10.1111/acel.12353

74. Chianelli M, Mather SJ, Grossman A, Sobnak R, Fritzberg A, Britton KE, et al. 99mTc-interleukin-2 scintigraphy in normal subjects and in patients with autoimmune thyroid diseases: a feasibility study. *Eur J Nucl Med Mol Imaging.* (2008) 35:2286–93. doi: 10.1007/s00259-008-0837-7

75. Telenga ED, van der Bij W, de Vries EFJ, Verschuuren EAM, Timens W, Luurtsema G, et al. 99m Tc-HYNIC-IL-2 scintigraphy to detect acute rejection in lung transplantation patients: a proof-of-concept study. *EJNMMI Res.* (2019) 9:41. doi: 10.1186/s13550-019-0511-z

76. Glaudemans AWJM, Bonanno E, Galli F, Zeebregts CJ, De Vries EFJ, Koole M, et al. *In vivo* and *in vitro* evidence that ^{99}mTc-HYNIC-interleukin-2 is able to detect T lymphocytes in vulnerable atherosclerotic plaques of the carotid artery. *Eur J Nucl Med Mol Imaging.* (2014) 41:1710–9. doi: 10.1007/s00259-014-2764-0

77. Lucia P, Parisella MG, Danese C, Bruno F, Manetti LL, Capriotti G, et al. Diagnosis and followup of Takayasu's arteritis by scintigraphy with radiolabelled interleukin 2. *J Rheumatol.* (2004) 31:1225–7.

78. Verhoeff SR, van den Heuvel MM, van Herpen CML, Piet B, Aarntzen EHJG, Heskamp S. Programmed cell death-1/ligand-1 PET imaging: a novel tool to optimize immunotherapy? *PET Clin.* (2020) 15:35–43. doi: 10.1016/j.cpet.2019.08.008

79. Cadena RH, Abdulahad WH, Hospers GAP, Wind TT, Boots AMH, Heeringa P, et al. Checks and balances in autoimmune vasculitis. *Front Immunol.* (2018) 9:315. doi: 10.3389/fimmu.2018.00315

80. Van Der Geest KSM, Sandovici M, Rutgers A, Hiltermann TJN, Oosting SF, Slart RHJA, et al. Imaging in immune checkpoint inhibitor-induced polymyalgia rheumatica. *Ann Rheum Dis.* (2020). doi: 10.1136/annrheumdis-2020-217381. [Epub ahead of print].

81. Grebinoski S, Vignali DA. Inhibitory receptor agonists: the future of autoimmune disease therapeutics? *Curr Opin Immunol.* (2020) 67:1–9. doi: 10.1016/j.coi.2020.06.001

82. Helou DG, Shafiei-Jahani P, Lo R, Howard E, Hurrell BP, Galle-Treger L, et al. PD-1 pathway regulates ILC2 metabolism and PD-1 agonist treatment ameliorates airway hyperreactivity. *Nat Commun.* (2020) 11:1–15. doi: 10.1038/s41467-020-17813-1

83. Bryan CM, Rocklin GJ, Bick MJ, Ford A, Majri-Morrison S, Kroll AV, et al. Computational design of a synthetic PD-1 agonist. *Proc Natl Acad Sci USA.* (2021) 118:e2102164118. doi: 10.1073/pnas.2102164118

84. Curnock AP, Bossi G, Kumaran J, Bawden LJ, Figueiredo R, Tawar R, et al. Cell-targeted PD-1 agonists that mimic PD-L1 are potent T cell inhibitors. *JCI Insight.* (2021) 6:e152468. doi: 10.1172/jci.insight.152468

85. Charbonneau P, Syrota A, Crouzel C, Valois JM, Prenant C. Peripheral-type benzodiazepine receptors in the living heart characterized by positron emission tomography. *Circulation.* (1986) 73:476–83. doi: 10.1161/01.CIR.73.3.476

86. Hashimoto K, Inoue O, Suzuki K, Yamasaki T, Kojima M. Synthesis and evaluation of 11C-PK 11195 for in vivo study of peripheral-type benzodiazepine receptors using positron emission tomography. *Ann Nucl Med.* (1989) 3:63–71. doi: 10.1007/BF03164587

87. Gerhard A, Neumaier B, Elitok E, Glatting G, Ries V, Tomczak R, et al. *In vivo* imaging of activated microglia using [11C]PK11195 and positron emission tomography in patients after ischemic stroke. *Neuroreport.* (2000) 11:2957–60. doi: 10.1097/00001756-200009110-00025

88. Gaemperli O, Shalhoub J, Owen DRJ, Lamare F, Johansson S, Fouladi N, et al. Imaging intraplaque inflammation in carotid atherosclerosis with 11C-PK11195 positron emission tomography/computed tomography. *Eur Heart J.* (2012) 33:1902–10. doi: 10.1093/eurheartj/ehr367

89. Ammirati E, Moroni F, Magnoni M, Busnardo E, Di Terlizzi S, Villa C, et al. Carotid artery plaque uptake of 11 C-PK11195 inversely correlates with circulating monocytes and classical CD14 ++ CD16 - monocytes expressing HLA-DR. *Int J Cardiol Hear Vasc.* (2018) 21:32–5. doi: 10.1016/j.ijcha.2018.09.005

90. van den Ameele J, Hong YT, Manavaki R, Kouli A, Biggs H, MacIntyre Z, et al. [11C]PK11195-PET brain imaging of the mitochondrial translocator protein in mitochondrial disease. *Neurology.* (2021) 96:e2761–73. doi: 10.1212/WNL.0000000000012033

91. Debruyne JC, Van Laere KJ, Versijpt J, De Vos F, Eng JK, Strijckmans K, et al. Semiquantification of the peripheral-type benzodiazepine ligand [11C]PK11195 in normal human brain and application in multiple sclerosis patients. *Acta Neurol Belg.* (2002) 102:127–35.

92. Groom GN, Junck L, Foster NL, Frey KA, Kuhl DE, PET. of peripheral benzodiazepine binding sites in the microgliosis of Alzheimer's disease. *J Nucl Med.* (1995) 36:2207–10.

93. Pappata S, Cornu P, Samson Y, Prenant C, Benavides J, Scatton B, et al. study of carbon-11-PK 11195 binding to peripheral type benzodiazepine sites in glioblastoma: a case report. *J Nucl Med.* (1991) 32:1608–10.

94. Pugliese F, Gaemperli O, Kinderlerer AR, Lamare F, Shalhoub J, Davies AH, et al. Imaging of vascular inflammation with [11C]-PK11195 and positron emission tomography/computed tomography angiography. *J Am Coll Cardiol.* (2010) 56:653–61. doi: 10.1016/j.jacc.2010.02.063

95. Shah F, Hume SP, Pike VW, Ashworth S, McDermott J. Synthesis of the enantiomers of [N-methyl-11C]PK 11195 and comparison of their behaviours as radioligands for PK binding sites in rats. *Nucl Med Biol.* (1994) 21:573–81. doi: 10.1016/0969-8051(94)90022-1

96. Banati RB, Goerres GW, Myers R, Gunn RN, Turkheimer FE, Kreutzberg GW, et al. [11C](R)-PK11195 positron emission tomography imaging of activated microglia *in vivo* in Rasmussen's encephalitis. *Neurology.* (1999) 53:2199–203. doi: 10.1212/WNL.53.9.2199

97. Pavese N, Gerhard A, Tai YF, Ho AK, Turkheimer F, Barker RA, et al. Microglial activation correlates with severity in Huntington disease: a clinical and PET study. *Neurology.* (2006) 66:1638–43. doi: 10.1212/01.wnl.0000222734.56412.17

98. Van Der Laken CJ, Elzinga EH, Kropholler MA, Molthoff CFM, Van Der Heijden JW, Maruyama K, et al. Noninvasive imaging of macrophages in rheumatoid synovitis using 11C-(R)-PK11195 and positron emission tomography. *Arthritis Rheum.* (2008) 58:3350–5. doi: 10.1002/art.23955

99. Kropholler MA, Boellaard R, Elzinga EH, Van Der Laken CJ, Maruyama K, Kloet RW, et al. Quantification of (R)-[11C]PK11195 binding in rheumatoid arthritis. *Eur J Nucl Med Mol Imaging.* (2009) 36:624–31. doi: 10.1007/s00259-008-0987-7

100. Gent YYJ, Voskuyl AE, Kloet RW, Van Schaardenburg D, Hoekstra OS, Dijkmans BAC, et al. Macrophage positron emission tomography imaging as a biomarker for preclinical rheumatoid arthritis: findings of a prospective pilot study. *Arthritis Rheum.* (2012) 64:62–6. doi: 10.1002/art.30655

101. Nakatomi Y, Mizuno K, Ishii A, Wada Y, Tanaka M, Tazawa S, et al. Neuroinflammation in patients with chronic fatigue syndrome/myalgic encephalomyelitis: an ^{11}C-(R)-PK11195 PET study. *J Nucl Med.* (2014) 55:945–50. doi: 10.2967/jnumed.113.131045

102. Haarman BCMB, Riemersma-Van der Lek RF, de Groot JC, Ruhé HGE, Klein HC, Zandstra TE, et al. Neuroinflammation in bipolar disorder - A [(11)C]-(R)-PK11195 positron emission tomography study. *Brain Behav Immun.* (2014) 40:219–25. doi: 10.1016/j.bbi.2014.03.016

103. Gent YYJ, ter Wee MM, Voskuyl AE, den Uyl D, Ahmadi N, Dowling C, et al. Subclinical synovitis detected by macrophage PET, but not MRI, is related to short-term flare of clinical disease activity in early RA patients: an exploratory study. *Arthritis Res Ther.* (2015) 17:266. doi: 10.1186/s13075-015-0770-7

104. Jeon SY, Seo S, Lee JS, Choi SH, Lee DH, Jung YH, et al. [11C]-(R)-PK11195 positron emission tomography in patients with complex regional pain syndrome: a pilot study. *Medicine.* (2017) 96:e5735. doi: 10.1097/MD.0000000000005735

105. Seo S, Jung YH, Lee D, Lee WJ, Jang JH, Lee JY, et al. Abnormal neuroinflammation in fibromyalgia and CRPS using [11C]-(R)-PK11195 PET. *PLoS ONE.* (2021) 16:0246152. doi: 10.1371/journal.pone.0246152

106. Lamare F, Hinz R, Gaemperli O, Pugliese F, Mason JC, Spinks T, et al. Detection and quantification of large-vessel inflammation with 11C-(R)-PK11195 PET/CT. *J Nucl Med.* (2011) 52:33–9. doi: 10.2967/jnumed.110.079038

107. Banati RB, Newcombe J, Gunn RN, Cagnin A, Turkheimer F, Heppner F, et al. The peripheral benzodiazepine binding site in the brain in multiple sclerosis: quantitative in vivo imaging of microglia as a measure of disease activity. *Brain.* (2000) 123:2321–37. doi: 10.1093/brain/123.11.2321

108. Cagnin A, Myers R, Gunn RN, Lawrence AD, Stevens T, Kreutzberg GW, et al. In vivo visualization of activated glia by [11C] (R)-PK11195-PET following herpes encephalitis reveals projected neuronal damage beyond the primary focal lesion. *Brain.* (2001) 124:2014–27. doi: 10.1093/brain/124.10.2014

109. Gerhard A, Banati RB, Goerres GB, Cagnin A, Myers R, Gunn RN, et al. [11C](R)-PK11195 PET imaging of microglial activation in multiple system atrophy. *Neurology.* (2003) 61:686–9. doi: 10.1212/01.WNL.0000078192.95645.E6

110. Turner MR, Cagnin A, Turkheimer FE, Miller CCJ, Shaw CE, Brooks DJ, et al. Evidence of widespread cerebral microglial activation in amyotrophic lateral sclerosis: an [11C](R)-PK11195 positron emission tomography study. *Neurobiol Dis.* (2004) 15:601–9. doi: 10.1016/j.nbd.2003.12.012

111. Gerhard A, Schwarz J, Myers R, Wise R, Banati RB. Evolution of microglial activation in patients after ischemic stroke: a [11C](R)-PK11195 PET study. *Neuroimage.* (2005) 24:591–5. doi: 10.1016/j.neuroimage.2004.09.034

112. Hammoud DA, Endres CJ, Chander AR, Guilarte TR, Wong DF, Sacktor NC, et al. Imaging glial cell activation with [11C]-R-PK11195 in patients with AIDS. *J Neurovirol.* (2005) 11:346–55. doi: 10.1080/13550280500187351

113. Gerhard A, Pavese N, Hotton G, Turkheimer F, Es M, Hammers A, et al. In vivo imaging of microglial activation with [11C](R)-PK11195 PET in idiopathic Parkinson's disease. *Neurobiol Dis.* (2006) 21:404–12. doi: 10.1016/j.nbd.2005.08.002

114. Cagnin A, Taylor-Robinson SD, Forton DM, Banati RB. In vivo imaging of cerebral "peripheral benzodiazepine binding sites" in patients with hepatic encephalopathy. *Gut.* (2006) 55:547–53. doi: 10.1136/gut.2005.075051

115. Brody AL, Gehlbach D, Garcia LY, Enoki R, Hoh C, Vera D, et al. Effect of overnight smoking abstinence on a marker for microglial activation: a [11C]DAA1106 positron emission tomography study. *Psychopharmacology.* (2018) 235:3525–34. doi: 10.1007/s00213-018-5077-3

116. Brody AL, Okita K, Shieh J, Liang L, Hubert R, Mamoun M, et al. Radiation dosimetry and biodistribution of the translocator protein radiotracer [(11)C]DAA1106 determined with PET/CT in healthy human volunteers. *Nucl Med Biol.* (2014) 41:871–5. doi: 10.1016/j.nucmedbio.2014.07.004

117. Yasuno F, Kosaka J, Ota M, Higuchi M, Ito H, Fujimura Y, et al. Increased binding of peripheral benzodiazepine receptor in mild cognitive impairment-dementia converters measured by positron emission tomography with [¹¹C]DAA1106. *Psychiatry Res.* (2012) 203:67–74. doi: 10.1016/j.pscychresns.2011.08.013

118. Takano A, Arakawa R, Ito H, Tateno A, Takahashi H, Matsumoto R, et al. Peripheral benzodiazepine receptors in patients with chronic schizophrenia: a PET study with [11C]DAA1106. *Int J Neuropsychopharmacol.* (2010) 13:943–50. doi: 10.1017/S1461145710000313

119. Yasuno F, Ota M, Kosaka J, Ito H, Higuchi M, Doronbekov TK, et al. Increased binding of peripheral benzodiazepine receptor in Alzheimer's disease measured by positron emission tomography with [11C]DAA1106. *Biol Psychiatry.* (2008) 64:835–41. doi: 10.1016/j.biopsych.2008.04.021

120. Ikoma Y, Yasuno F, Ito H, Suhara T, Ota M, Toyama H, et al. Quantitative analysis for estimating binding potential of the peripheral benzodiazepine receptor with [(11)C]DAA1106. *J Cereb Blood Flow Metab.* (2007) 27:173–84. doi: 10.1038/sj.jcbfm.9600325

121. Zhang MR Kida T, Noguchi J, Furutsuka K, Maeda J, Suhara T, Suzuki K. [(11)C]DAA1106: radiosynthesis and in vivo binding to peripheral benzodiazepine receptors in mouse brain. *Nucl Med Biol.* (2003) 30:513–9. doi: 10.1016/S0969-8051(03)00016-7

122. Schroeder DC, Popp E, Rohleder C, Vus S, de la Bethencourt DP, Finke SR, et al. Positron emission tomography imaging of long-term expression of the 18 kDa translocator protein after sudden cardiac arrest in rats. *Shock.* (2021) 55:620–9. doi: 10.1097/SHK.0000000000001546

123. Wang M, Gao M, Zheng QH. Fully automated synthesis of PET TSPO radioligands [11C]DAA1106 and [18F]FEDAA1106. *Appl Radiat Isot.* (2012) 70:965–73. doi: 10.1016/j.apradiso.2012.03.011

124. Kumata K, Zhang Y, Fujinaga M, Ohkubo T, Mori W, Yamasaki T, et al. [18F]DAA1106: automated radiosynthesis using spirocyclic iodonium ylide and preclinical evaluation for positron emission tomography imaging of translocator protein (18 kDa). *Bioorg Med Chem.* (2018) 26:4817–22. doi: 10.1016/j.bmc.2018.08.017

125. Zhang MR, Maeda J, Furutsuka K, Yoshida Y, Ogawa M, Suhara T, et al. [18F]FMDAA1106 and [18F]FEDAA1106: two positron-emitter labeled ligands for peripheral benzodiazepine receptor (PBR). *Bioorg Med Chem Lett.* (2003) 13:201–4. doi: 10.1016/S0960-894X(02)00886-7

126. Fujimura Y, Ikoma Y, Yasuno F, Suhara T, Ota M, Matsumoto R, et al. Quantitative analyses of 18F-FEDAA1106 binding to peripheral benzodiazepine receptors in living human brain. *J Nucl Med.* (2006) 47:43–50.

127. Cuhlmann S, Gsell W, Van Der Heiden K, Habib J, Tremoleda JL, Khalil M, et al. In vivo mapping of vascular inflammation using the translocator protein tracer 18F-FEDAA1106. *Mol Imaging.* (2014) 13:1–11. doi: 10.2310/7290.2014.00014

128. Takano A, Piehl F, Hillert J, Varrone A, Nag S, Gulyás B, et al. In vivo TSPO imaging in patients with multiple sclerosis: a brain PET study with [18F]FEDAA1106. *EJNMMI Res.* (2013) 3:1–9. doi: 10.1186/2191-219X-3-30

129. Varrone A, Mattsson P, Forsberg A, Takano A, Nag S, Gulyàs B, et al. In vivo imaging of the 18-kDa translocator protein (TSPO) with [18F]FEDAA1106 and PET does not show increased binding in Alzheimer's disease patients. *Eur J Nucl Med Mol Imaging.* (2013) 40:921–31. doi: 10.1007/s00259-013-2359-1

130. Takano A, Gulyás B, Varrone A, Karlsson P, Sjoholm N, Larsson S, et al. Biodistribution and radiation dosimetry of the 18 kDa translocator protein (TSPO) radioligand [18F]FEDAA1106: a human whole-body PET study. *Eur J Nucl Med Mol Imaging.* (2011) 38:2058–65. doi: 10.1007/s00259-011-1864-3

131. Pascual B, Funk Q, Zanotti-Fregonara P, Cykowski MD, Veronese M, Rockers E, et al. Neuroinflammation is highest in areas of disease progression in semantic dementia. *Brain.* (2021) 144:1565–75. doi: 10.1093/brain/awab057

132. Klein J, Yan X, Johnson A, Tomljanovic Z, Zou J, Polly K, et al. Olfactory impairment is related to tau pathology and neuroinflammation in Alzheimer's disease. *J Alzheimers Dis.* (2021) 80:1051–65. doi: 10.3233/JAD-201149

133. Dimber R, Guo Q, Bishop C, Adonis A, Buckley A, Kocsis A, et al. Evidence of brain inflammation in patients with human T-lymphotropic virus type 1-associated myelopathy (HAM): a pilot, multimodal imaging study using 11C-PBR28 PET, MR T1-weighted, and diffusion-weighted imaging. *J Nucl Med.* (2016) 57:1905–12. doi: 10.2967/jnumed.116.175083

134. Park E, Gallezot JD, Delgadillo A, Liu S, Planeta B, Lin SF, et al. (11)C-PBR28 imaging in multiple sclerosis patients and healthy controls: test-retest reproducibility and focal visualization of active white matter areas. *Eur J Nucl Med Mol Imaging.* (2015) 42:1081–92. doi: 10.1007/s00259-015-3043-4

135. Fujita M, Imaizumi M, Zoghbi SS, Fujimura Y, Farris AG, Suhara T, et al. Kinetic analysis in healthy humans of a novel positron emission tomography radioligand to image the peripheral benzodiazepine receptor, a potential biomarker for inflammation. *Neuroimage.* (2008) 40:43–52. doi: 10.1016/j.neuroimage.2007.11.011

136. Brown AK, Fujita M, Fujimura Y, Liow JS, Stabin M, Ryu YH, et al. Radiation dosimetry and biodistribution in monkey and man of 11C-PBR28: a PET radioligand to image inflammation. *J Nucl Med.* (2007) 48:2072–9. doi: 10.2967/jnumed.107.044842

137. Imaizumi M, Kim HJ, Zoghbi SS, Briard E, Hong J, Musachio JL, et al. PET imaging with [11C]PBR28 can localize and quantify upregulated peripheral benzodiazepine receptors associated with cerebral ischemia in rat. *Neurosci Lett.* (2007) 411:200–5. doi: 10.1016/j.neulet.2006.09.093

138. Tran TT, Gallezot JD, Jilaveanu LB, Zito C, Turcu G, Lim K, et al. [11C]Methionine and [11C]PBR28 as PET imaging tracers to differentiate metastatic tumor recurrence or radiation necrosis. *Mol Imaging.* (2020) 19:1–9. doi: 10.1177/1536012120968669

139. Boerwinkle AH, Strain JF, Burdo T, Doyle J, Christensen J, Su Y, et al. Comparison of [11C]-PBR28 binding between persons living with HIV and HIV-uninfected individuals. *J Acquir Immune Defic Syndr.* (2020) 85:244–51. doi: 10.1097/QAI.0000000000002435

140. Dani M, Wood M, Mizoguchi R, Fan Z, Walker Z, Morgan R, et al. Microglial activation correlates in vivo with both tau and amyloid in Alzheimer's disease. *Brain.* (2018) 141:2740–54. doi: 10.1093/brain/awy188

141. Alshikho MJ, Zürcher NR, Loggia ML, Cernasov P, Reynolds B, Pijanowski O, et al. Integrated magnetic resonance imaging and [11C]-PBR28 positron emission tomographic imaging in amyotrophic lateral sclerosis. *Ann Neurol.* (2018) 83:1186–97. doi: 10.1002/ana.25251

142. Lois C, González I, Izquierdo-García D, Zürcher NR, Wilkens P, Loggia ML, et al. Neuroinflammation in Huntington's disease: new insights with 11C-PBR28 PET/MRI. *ACS Chem Neurosci.* (2018) 9:2563–71. doi: 10.1021/acschemneuro.8b00072

143. Paganoni S, Alshikho MJ, Zürcher NR, Cernasov P, Babu S, Loggia ML, et al. Imaging of glia activation in people with primary lateral sclerosis. *NeuroImage Clin.* (2017) 17:347–53. doi: 10.1016/j.nicl.2017.10.024

144. Ran C, Albrecht DS, Bredella MA, Yang J, Yang J, Liang SH, et al. Imaging of human brown adipose tissue with the TSPO Tracer [11C]PBR28. *Mol Imaging Biol.* (2018) 20:188–93. doi: 10.1007/s11307-017-1129-z

145. Veronese M, Reis Marques T, Bloomfield PS, Rizzo G, Singh N, Jones D, et al. Kinetic modelling of [11C]PBR28 for 18 kDa translocator protein PET data: a validation study of vascular modelling in the brain using XBD173 and tissue analysis. *J Cereb Blood Flow Metab.* (2018) 38:1227–42. doi: 10.1177/0271678X17712388

146. Singhal T, O'Connor K, Dubey S, Belanger AP, Hurwitz S, Chu R, et al. 18F-PBR06 versus 11C-PBR28 PET for assessing white matter translocator protein binding in multiple sclerosis. *Clin Nucl Med.* (2018) 43:e289–95. doi: 10.1097/RLU.0000000000002179

147. Wang M, Gao M, Miller KD, Zheng QH. Synthesis of [11C]PBR06 and [18F]PBR06 as agents for positron emission tomographic (PET) imaging of the translocator protein (TSPO). *Steroids.* (2011) 76:1331–40. doi: 10.1016/j.steroids.2011.06.012

148. Dickstein LP, Zoghbi SS, Fujimura Y, Imaizumi M, Zhang Y, Pike VW, et al. Comparison of 18F- and 11C-labeled aryloxyanilide analogs to measure translocator protein in human brain using positron emission tomography. *Eur J Nucl Med Mol Imaging.* (2011) 38:352–7. doi: 10.1007/s00259-010-1622-y

149. Fujimura Y, Kimura Y, Si?eon FG, Dickstein LP, Pike VW, Innis RB, et al. Biodistribution and radiation dosimetry in humans of a new PET ligand, (18)F-PBR06, to image translocator protein (18 kDa). *J Nucl Med.* (2010) 51:145–9. doi: 10.2967/jnumed.109.068064

150. Fujimura Y, Zoghbi SS, Simèon FG, Taku A, Pike VW, Innis RB, et al. Quantification of translocator protein (18 kDa) in the human brain with PET and a novel radioligand, (18)F-PBR06. *J Nucl Med.* (2009) 50:1047–53. doi: 10.2967/jnumed.108.060186

151. Imaizumi M, Briard E, Zoghbi SS, Gourley JP, Hong J, Musachio JL, et al. Kinetic evaluation in nonhuman primates of two new PET ligands for peripheral benzodiazepine receptors in brain. *Synapse.* (2007) 61:595–605. doi: 10.1002/syn.20394

152. Briard E, Zoghbi SS, Imaizumi M, Gourley JP, Shetty HU, Hong J, et al. Synthesis and evaluation in monkey of two sensitive 11C-labeled aryloxyanilide ligands for imaging brain peripheral benzodiazepine receptors in vivo. *J Med Chem.* (2008) 51:17–30. doi: 10.1021/jm0707370

153. Wilson AA, Garcia A, Parkes J, McCormick P, Stephenson KA, Houle S, et al. Radiosynthesis and initial evaluation of [18F]-FEPPA for PET imaging of peripheral benzodiazepine receptors. *Nucl Med Biol.* (2008) 35:305–14. doi: 10.1016/j.nucmedbio.2007.12.009

154. Rusjan PM, Wilson AA, Bloomfield PM, Vitcu I, Meyer JH, Houle S, et al. Quantitation of translocator protein binding in human brain with the novel radioligand [18F]-FEPPA and positron emission tomography. *J Cereb Blood Flow Metab.* (2011) 31:1807–16. doi: 10.1038/jcbfm.2011.55

155. Suridjan I, Rusjan PM, Kenk M, Verhoeff NPLG, Voineskos AN, Rotenberg D, et al. Quantitative imaging of neuroinflammation in human white matter: a positron emission tomography study with translocator protein 18 kDa radioligand, [18F]-FEPPA. *Synapse.* (2014) 68:536–47. doi: 10.1002/syn.21765

156. Mizrahi R, Rusjan PM, Vitcu I, Ng A, Wilson AA, Houle S, et al. Whole body biodistribution and radiation dosimetry in humans of a new PET ligand, [(18)F]-FEPPA, to image translocator protein (18 kDa). *Mol imaging Biol.* (2013) 15:353–9. doi: 10.1007/s11307-012-0589-4

157. Suridjan I, Rusjan PM, Voineskos AN, Selvanathan T, Setiawan E, Strafella AP, et al. Neuroinflammation in healthy aging: a PET study using a novel Translocator Protein 18kDa (TSPO) radioligand, [(18)F]-FEPPA. *Neuroimage.* (2014) 84:868–75. doi: 10.1016/j.neuroimage.2013.09.021

158. Kenk M, Selvanathan T, Rao N, Suridjan I, Rusjan P, Remington G, et al. Imaging neuroinflammation in gray and white matter in schizophrenia: an in-vivo PET study with [18F]-FEPPA. *Schizophr Bull.* (2015) 41:85–93. doi: 10.1093/schbul/sbu157

159. Suridjan I, Pollock BG, Verhoeff NPLG, Voineskos AN, Chow T, Rusjan PM, et al. In-vivo imaging of grey and white matter neuroinflammation in Alzheimer's disease: a positron emission tomography study with a novel radioligand, [18F]-FEPPA. *Mol Psychiatry.* (2015) 20:1579–87. doi: 10.1038/mp.2015.1

160. Koshimori Y, Ko JH, Mizrahi R, Rusjan P, Mabrouk R, Jacobs MF, et al. Imaging striatal microglial activation in patients with Parkinson's Disease. *PLoS ONE.* (2015) 10:138721. doi: 10.1371/journal.pone.0138721

161. Hafizi S, Tseng HH, Rao N, Selvanathan T, Kenk M, Bazinet RP, et al. Imaging microglial activation in untreated first-episode psychosis: a PET study with [18F]FEPPA. *Am J Psychiatry.* (2017) 174:118–24. doi: 10.1176/appi.ajp.2016.16020171

162. Attwells S, Setiawan E, Wilson AA, Rusjan PM, Mizrahi R, Miler L, et al. Inflammation in the neurocircuitry of obsessive-compulsive disorder. *JAMA Psychiatry.* (2017) 74:833–40. doi: 10.1001/jamapsychiatry.2017.1567

163. Rathitharan G, Truong J, Tong J, McCluskey T, Meyer JH, Mizrahi R, et al. Microglia imaging in methamphetamine use disorder: a positron emission tomography study with the 18 kDa translocator protein radioligand [F-18]FEPPA. *Addict Biol.* (2021) 26:e12876. doi: 10.1111/adb.12876

164. Ottoy J, De Picker L, Verhaeghe J, Deleye S, Wyffels L, Kosten L, et al. 18 F-PBR111 PET imaging in healthy controls and schizophrenia: test-retest reproducibility and quantification of neuroinflammation. *J Nucl Med.* (2018) 59:1267–74. doi: 10.2967/jnumed.117.203315

165. Guo Q, Colasanti A, Owen DR, Onega M, Kamalakaran A, Bennacef I, et al. Quantification of the specific translocator protein signal of 18F-PBR111 in healthy humans: a genetic polymorphism effect on in vivo binding. *J Nucl Med.* (2013) 54:1915–23. doi: 10.2967/jnumed.113.121020

166. Bourdier T, Pham TQ, Henderson D, Jackson T, Lam P, Izard M, et al. Automated radiosynthesis of [18F]PBR111 and [18F]PBR102 using the Tracerlab FXFN and Tracerlab MXFDG module for imaging the peripheral benzodiazepine receptor with PET. *Appl Radiat Isot.* (2012) 70:176–83. doi: 10.1016/j.apradiso.2011.07.014

167. Van Camp N, Boisgard R, Kuhnast B, Thézé B, Viel T, Grégoire MC, et al. In vivo imaging of neuroinflammation: a comparative study between [(18)F]PBR111, [(11)C]CLINME and [(11)C]PK11195 in an acute rodent model. *Eur J Nucl Med Mol Imaging.* (2010) 37:962–72. doi: 10.1007/s00259-009-1353-0

168. Datta G, Colasanti A, Kalk N, Owen D, Scott G, Rabiner EA, et al. 11 C-PBR28 and 18 F-PBR111 detect white matter inflammatory

heterogeneity in multiple sclerosis. *J Nucl Med.* (2017) 58:1477–82. doi: 10.2967/jnumed.116.187161

169. Fookes CJR, Pham TQ, Mattner F, Greguric I, Loc'h C, Liu X, et al. Synthesis and biological evaluation of substituted [18F]imidazo[1,2-a]pyridines and [18F]pyrazolo[1,5-a]pyrimidines for the study of the peripheral benzodiazepine receptor using positron emission tomography. *J Med Chem.* (2008) 51:3700–12. doi: 10.1021/jm7014556

170. Verschuer JD, Towson J, Eberl S, Katsifis A, Henderson D, Lam P, et al. Radiation dosimetry of the translocator protein ligands [18F]PBR111 and [18F]PBR102. *Nucl Med Biol.* (2012) 39:742–53. doi: 10.1016/j.nucmedbio.2011.11.003

171. Ishibashi K, Miura Y, Imamura A, Toyohara J, Ishii K. Microglial activation on 11C-CB184 PET in a patient with cerebellar ataxia associated with HIV infection. *Clin Nucl Med.* (2018) 43:e82–4. doi: 10.1097/RLU.0000000000001936

172. Sakata M, Ishibashi K, Imai M, Wagatsuma K, Ishii K, Hatano K, et al. Assessment of safety, efficacy, and dosimetry of a novel 18-kDa translocator protein ligand, [11C]CB184, in healthy human volunteers. *EJNMMI Res.* (2017) 7:26. doi: 10.1186/s13550-017-0271-6

173. Toyohara J, Sakata M, Hatano K, Yanai S, Endo S, Ishibashi K, et al. Preclinical and first-in-man studies of [(11C)CB184 for imaging the 18-kDa translocator protein by positron emission tomography. *Ann Nucl Med.* (2016) 30:534–43. doi: 10.1007/s12149-016-1094-7

174. Hatano K, Sekimata K, Yamada T, Abe J, Ito K, Ogawa M, et al. Radiosynthesis and *in vivo* evaluation of two imidazopyridineacetamides, [(11C)CB184 and [(11C)CB190, as a PET tracer for 18 kDa translocator protein: direct comparison with [(11C)(R)-PK11195. *Ann Nucl Med.* (2015) 29:325–35. doi: 10.1007/s12149-015-0948-8

175. Boutin H, Chauveau F, Thominiaux C, Kuhnast B, Grégoire MC, Jan S, et al. In vivo imaging of brain lesions with [(11C)CLINME, a new PET radioligand of peripheral benzodiazepine receptors. *Glia.* (2007) 55:1459–68. doi: 10.1002/glia.20562

176. Doorduin J, de Vries E, Dierckx R, Klein H, PET. imaging of the peripheral benzodiazepine receptor: monitoring disease progression and therapy response in neurodegenerative disorders. *Curr Pharm Des.* (2008) 14:3297–315. doi: 10.2174/138161208786549443

177. Perrone M, Moon BS, Park HS, Laquintana V, Jung JH, Cutrignelli A, et al. A novel PET imaging probe for the detection and monitoring of translocator protein 18 kDa expression in pathological disorders. *Sci Rep.* (2016) 6:20422. doi: 10.1038/srep20422

178. Kim GR, Paeng JC, Jung JH, Moon BS, Lopalco A, Denora N, Lee BC, Kim SE. Assessment of TSPO in a rat experimental autoimmune myocarditis model: a comparison study between [18F]fluoromethyl-PBR28 and [18F]CB251. *Int J Mol Sci.* (2018) 19:276. doi: 10.3390/ijms19010276

179. Kim K, Kim H, Bae SH, Lee SY, Kim YH, Na J, et al. [18F]CB251 PET/MR imaging probe targeting translocator protein (TSPO) independent of its polymorphism in a neuroinflammation model. *Theranostics.* (2020) 10:9315–31. doi: 10.7150/thno.46875

180. Amitani M, Zhang MR, Noguchi J, Kumata K, Ito T, Takai N, et al. Blood flow dependence of the intratumoral distribution of peripheral benzodiazepine receptor binding in intact mouse fibrosarcoma. *Nucl Med Biol.* (2006) 33:971–5. doi: 10.1016/j.nucmedbio.2006.08.004

181. Yui J, Hatori A, Kawamura K, Yanamoto K, Yamasaki T, Ogawa M, et al. Visualization of early infarction in rat brain after ischemia using a translocator protein (18 kDa) PET ligand [11C]DAC with ultra-high specific activity. *Neuroimage.* (2011) 54:123–30. doi: 10.1016/j.neuroimage.2010.08.010

182. Yanamoto K, Yamasaki T, Kumata K, Yui J, Odawara C, Kawamura K, et al. Evaluation of N-benzyl-N-[11C]methyl-2- (7-methyl-8-oxo-2-phenyl-7,8-dihydro-9H-purin-9-yl)acetamide ([11C]DAC) as a novel translocator protein (18 kDa) radioligand in kainic acid-lesioned rat. *Synapse.* (2009) 63:961–71. doi: 10.1002/syn.20678

183. James ML, Fulton RR, Henderson DJ, Eberl S, Meikle SR, Thomson S, et al. Synthesis and *in vivo* evaluation of a novel peripheral benzodiazepine receptor PET radioligand. *Bioorg Med Chem.* (2005) 13:6188–94. doi: 10.1016/j.bmc.2005.06.030

184. Boutin H, Chauveau F, Thominiaux C, Grégoire MC, James ML, Trebossen R, et al. 11C-DPA-713: a novel peripheral benzodiazepine receptor PET ligand for *in vivo* imaging of neuroinflammation. *J Nucl Med.* (2007) 48:573–81. doi: 10.2967/jnumed.106.036764

185. Yaqub M, Verweij NJF, Pieplenbosch S, Boellaard R, Lammertsma AA, Van Der Laken CJ. Quantitative assessment of arthritis activity in rheumatoid arthritis patients using [11C]DPA-713 positron emission tomography. *Int J Mol Sci.* (2020) 21:3137. doi: 10.3390/ijms21093137

186. Endres CJ, Pomper MG, James M, Uzuner O, Hammoud DA, Watkins CC, et al. Initial evaluation of 11C-DPA-713, a novel TSPO PET ligand, in humans. *J Nucl Med.* (2009) 50:1276–82. doi: 10.2967/jnumed.109.062265

187. Endres CJ, Coughlin JM, Gage KL, Watkins CC, Kassiou M, Pomper MG. Radiation dosimetry and biodistribution of the TSPO ligand 11C-DPA-713 in humans. *J Nucl Med.* (2012) 53:330–5. doi: 10.2967/jnumed.111.094565

188. Coughlin JM, Wang Y, Ma S, Yue C, Kim PK, Adams A V, et al. Regional brain distribution of translocator protein using [(11C)DPA-713 PET in individuals infected with HIV. *J Neurovirol.* (2014) 20:219–32. doi: 10.1007/s13365-014-0239-5

189. Coughlin JM, Wang Y, Ambinder EB, Ward RE, Minn I, Vranesic M, et al. *In vivo* markers of inflammatory response in recent-onset schizophrenia: a combined study using [(11C)DPA-713 PET and analysis of CSF and plasma. *Transl Psychiatry.* (2016) 6:1–8. doi: 10.1038/tp.2016.40

190. Wang Y, Coughlin JM, Ma S, Endres CJ, Kassiou M, Sawa A, et al. Neuroimaging of translocator protein in patients with systemic lupus erythematosus: a pilot study using [11C]DPA-713 positron emission tomography. *Lupus.* (2017) 26:170–8. doi: 10.1177/0961203316657432

191. Rubin LH, Sacktor N, Creighton J, Du Y, Endres CJ, Pomper MG, et al. Microglial activation is inversely associated with cognition in individuals living with HIV on effective antiretroviral therapy. *AIDS.* (2018) 32:1661–7. doi: 10.1097/QAD.0000000000001858

192. Coughlin JM, Yang T, Rebman AW, Bechtold KT, Du Y, Mathews WB, et al. Imaging glial activation in patients with post-treatment Lyme disease symptoms: a pilot study using [11C]DPA-713 PET. *J Neuroinflamm.* (2018) 82:29–36. doi: 10.1186/s12974-018-1381-4

193. Bruijnen STG, Verweij NJF, Gent YYJ, Huisman MC, Windhorst AD, Kassiou M, et al. Imaging disease activity of rheumatoid arthritis by macrophage targeting using second generation translocator protein positron emission tomography tracers. *PLoS ONE.* (2019) 14:222844. doi: 10.1371/journal.pone.0222844

194. Lavisse S, Goutal S, Wimberley C, Tonietto M, Bottlaender M, Gervais P, et al. Increased microglial activation in patients with Parkinson disease using [18F]-DPA714 TSPO PET imaging. *Parkinsonism Relat Disord.* (2021) 82:29–36. doi: 10.1016/j.parkreldis.2020.11.011

195. James ML, Fulton RR, Vercoullie J, Henderson DJ, Garreau L, Chalon S, et al. DPA-714, a new translocator protein-specific ligand: synthesis, radiofluorination, and pharmacologic characterization. *J Nucl Med.* (2008) 49:814–22. doi: 10.2967/jnumed.107.046151

196. Médran-Navarrete V, Bernards N, Kuhnast B, Damont A, Pottier G, Peyronneau MA, et al. [18F]DPA-C5yne, a novel fluorine-18-labelled analogue of DPA-714: radiosynthesis and preliminary evaluation as a radiotracer for imaging neuroinflammation with PET. *J Labelled Comp Radiopharm.* (2014) 57:410–8. doi: 10.1002/jlcr.3199

197. López-Picón FR, Keller T, Bocancea D, Helin JS, Krzyczmonik A, Helin S, et al. Direct comparison of [18F]F-DPA with [18F]DPA-714 and [11C]PBR28 for neuroinflammation imaging in the same Alzheimer's disease model mice and healthy controls. *Mol imaging Biol.* (2022) 24:157–66. doi: 10.1007/s11307-021-01646-5

198. Mou T, Tian J, Tian Y, Yun M, Li J, Dong W, et al. Automated synthesis and preliminary evaluation of [18F]FDPA for cardiac inflammation imaging in rats after myocardial infarction. *Sci Rep.* (2020) 10:18685 doi: 10.1038/s41598-020-75705-2

199. Wang L, Cheng R, Fujinaga M, Yang J, Zhang Y, Hatori A, et al. A facile radiolabeling of [18F]FDPA via spirocyclic iodonium ylides: preliminary PET imaging studies in preclinical models of neuroinflammation. *J Med Chem.* (2017) 60:5222–7. doi: 10.1021/acs.jmedchem.7b00432

200. Keller T, Krzyczmonik A, Forsback S, Picón FRL, Kirjavainen AK, Takkinen J, et al. Radiosynthesis and preclinical evaluation of [18F]F-DPA, a novel pyrazolo[1,5a]pyrimidine acetamide TSPO radioligand, in healthy sprague dawley rats. *Mol imaging Biol.* (2017) 19:736–45. doi: 10.1007/s11307-016-1040-z

201. Tang D, Fujinaga M, Hatori A, Zhang Y, Yamasaki T, Xie L, et al. Evaluation of the novel TSPO radiotracer 2-(7-butyl-2-(4-(2-([18 F]fluoroethoxy)phenyl)-5-methylpyrazolo[1,5-a]pyrimidin-3-yl)-N,N-diethylacetamide in a preclinical model of neuroinflammation. *Eur J Med Chem.* (2018) 150:1–8. doi: 10.1016/j.ejmech.2018.02.076

202. Tang D, Li J, Nickels ML, Huang G, Cohen AS, Manning HC. Preclinical evaluation of a Novel TSPO PET Ligand 2-(7-Butyl-2-(4-(2-[18 F]Fluoroethoxy)phenyl)-5-Methylpyrazolo[1,5-a]Pyrimidin-3-yl)-N,N-Diethylacetamide (18 F-VUIIS1018A) to Image Glioma. *Mol imaging Biol.* (2019) 21:113–21. doi: 10.1007/s11307-018-1198-7

203. Yanamoto K, Kumata K, Yamasaki T, Odawara C, Kawamura K, Yui J, et al. [18F]FEAC and [18F]FEDAC: two novel positron emission tomography ligands for peripheral-type benzodiazepine receptor in the brain. *Bioorg Med Chem Lett.* (2009) 19:1707–10. doi: 10.1016/j.bmcl.2009.01.093

204. Maekawa K, Tsuji AB, Yamashita A, Sugyo A, Katoh C, Tang M, et al. Translocator protein imaging with 18 F-FEDAC-positron emission tomography in rabbit atherosclerosis and its presence in human coronary vulnerable plaques. *Atherosclerosis.* (2021) 337:7–17. doi: 10.1016/j.atherosclerosis.2021.10.003

205. Chung SJ, Yoon HJ, Youn H, Kim MJ, Lee YS, Jeong JM, et al. 18 F-FEDAC as a targeting agent for activated macrophages in DBA/1 mice with collagen-induced arthritis: comparison with 18 F-FDG. *J Nucl Med.* (2018) 59:839–45. doi: 10.2967/jnumed.117.200667

206. Chauveau F, Boutin H, Van Camp N, Thominiaux C, Hantraye P, Rivron L, et al. In vivo imaging of neuroinflammation in the rodent brain with [11C]SSR180575, a novel indoleacetamide radioligand of the translocator protein (18 kDa). *Eur J Nucl Med Mol Imaging.* (2011) 38:509–14. doi: 10.1007/s00259-010-1628-5

207. Damont A, Marguet F, Puech F, Dollé F. Synthesis and *in vitro* characterization of novel fluorinated derivatives of the TSPO 18 kDa ligand SSR180575. *Eur J Med Chem.* (2015) 101:736–45. doi: 10.1016/j.ejmech.2015.07.033

208. Khan W, Corben LA, Bilal H, Vivash L, Delatycki MB, Egan GF, et al. Neuroinflammation in the cerebellum and brainstem in Friedreich Ataxia: an [18F]-FEMPA PET Study. *Mov Disord.* (2022) 37:218–24. doi: 10.1002/mds.28825

209. Hellberg S, Silvola JMU, Kiugel M, Liljenbäck H, Savisto N, Li XG, et al. 18-kDa translocator protein ligand 18 F-FEMPA: biodistribution and uptake into atherosclerotic plaques in mice. *J Nucl Cardiol.* (2017) 24:862–71. doi: 10.1007/s12350-016-0527-y

210. Varrone A, Oikonen V, Forsberg A, Joutsa J, Takano A, Solin O, et al. Positron emission tomography imaging of the 18-kDa translocator protein (TSPO) with [18F]FEMPA in Alzheimer's disease patients and control subjects. *Eur J Nucl Med Mol Imaging.* (2015) 42:438–46. doi: 10.1007/s00259-014-2955-8

211. Fiorenza D, Nicolai E, Cavaliere C, Fiorino F, Esposito G, Salvatore M. Fully automated synthesis of novel TSPO PET imaging ligand [18 F]Fluoroethyltemazepam. *Molecules.* (2021) 26:2372. doi: 10.3390/molecules26082372

212. Ji B, Ono M, Yamasaki T, Fujinaga M, Zhang MR, Seki C, et al. Detection of Alzheimer's disease-related neuroinflammation by a PET ligand selective for glial versus vascular translocator protein. *J Cereb Blood Flow Metab.* (2021) 41:2076–89. doi: 10.1177/0271678X21992457

213. Tiwari AK Ji B, Yui J, Fujinaga M, Yamasaki T, Xie L, Luo R, et al. [18F]FEBMP: positron emission tomography imaging of TSPO in a model of neuroinflammation in rats, and *in vitro* autoradiograms of the human brain. *Theranostics.* (2015) 5:961–9. doi: 10.7150/thno.12027

214. Scott AP, Thomas P, Pattison DA, Francis L, Ridge P, Tey SK, Kennedy GA. [18 F]GE-180 PET/CT assessment of enterocytic translocator protein (TSPO) over-expression: a pilot study in gastrointestinal GVHD. *Bone Marrow Transplant.* (2022) 57:517–9. doi: 10.1038/s41409-022-01571-3

215. Hellberg S, Liljenbäck H, Eskola O, Morisson-Iveson V, Morrison M, Trigg W, et al. Positron emission tomography imaging of macrophages in atherosclerosis with 18 F-GE-180, a radiotracer for translocator protein (TSPO). *Contrast Media Mol Imaging.* (2018) 2018:9186902. doi: 10.1155/2018/9186902

216. Zanotti-Fregonara P, Pascual B, Rizzo G, Yu M, Pal N, Beers D, et al. Head-to-head comparison of 11 C-PBR28 and 18 F-GE180 for quantification of the translocator protein in the human brain. *J Nucl Med.* (2018) 59:1260–6. doi: 10.2967/jnumed.117.203109

217. Vomacka L, Albert NL, Lindner S, Unterrainer M, Mahler C, Brendel M, et al. TSPO imaging using the novel PET ligand [18 F]GE-180: quantification approaches in patients with multiple sclerosis. *EJNMMI Res.* (2017) 7:89. doi: 10.1186/s13550-017-0340-x

218. Fan Z, Calsolaro V, Atkinson RA, Femminella GD, Waldman A, Buckley C, et al. Flutriciclamide (18F-GE180) PET: first-in-human PET study of novel third-generation *in vivo* marker of human translocator protein. *J Nucl Med.* (2016) 57:1753–9. doi: 10.2967/jnumed.115.169078

219. Feeney C, Scott G, Raffel J, Roberts S, Coello C, Jolly A, et al. Kinetic analysis of the translocator protein positron emission tomography ligand [18 F]GE-180 in the human brain. *Eur J Nucl Med Mol Imaging.* (2016) 43:2201–10. doi: 10.1007/s00259-016-3444-z

220. Wadsworth H, Jones PA, Chau WF, Durrant C, Fouladi N, Passmore J, et al. [18F]GE-180: a novel fluorine-18 labelled PET tracer for imaging Translocator protein 18 kDa (TSPO). *Bioorg Med Chem Lett.* (2012) 22:1308–13. doi: 10.1016/j.bmcl.2011.12.084

221. Vettermann FJ, Harris S, Schmitt J, Unterrainer M, Lindner S, Rauchmann BS, et al. Impact of TSPO receptor polymorphism on [18 F]GE-180 binding in healthy brain and pseudo-reference regions of neurooncological and neurodegenerative disorders. *Life.* (2021) 11:484. doi: 10.20944/preprints202104.0548.v1

222. Vainio SK, Dickens AM, Matilainen M, López-Picón FR, Aarnio R, Eskola O, et al. Dimethyl fumarate decreases short-term but not long-term inflammation in a focal EAE model of neuroinflammation. *EJNMMI Res.* (2022) 12:6. doi: 10.1186/s13550-022-00878-y

223. Qiao L, Fisher E, McMurray L, Milicevic Sephton S, Hird M, Kuzhuppilly-Ramakrishnan N, et al. Radiosynthesis of (R,S)-[18 F]GE387: a potential PET radiotracer for imaging translocator protein 18 kDa (TSPO) with low binding sensitivity to the human gene polymorphism rs6971. *ChemMedChem.* (2019) 14:982–93. doi: 10.1002/cmdc.201900023

224. Berroterán-Infante N, Kalina T, Fetty L, Janisch V, Velasco R, Vraka C, et al. (R)-[18 F]NEBIFQUINIDE: a promising new PET tracer for TSPO imaging. *Eur J Med Chem.* (2019) 176:410–8. doi: 10.1016/j.ejmech.2019.05.008

225. Rocha NP, Charron O, Latham LB, Colpo GD, Zanotti-Fregonara P, Yu M, et al. Microglia activation in basal ganglia is a late event in Huntington Disease pathophysiology. *Neurol Neuroimmunol Neuroinflamm.* (2021) 8:e984. doi: 10.1212/NXI.0000000000000984

226. Ikawa M, Lohith TG, Shrestha S, Telu S, Zoghbi SS, Castellano S, et al. 11C-ER176, a Radioligand for 18-kDa translocator protein, has adequate sensitivity to robustly image all three affinity genotypes in human brain. *J Nucl Med.* (2017) 58:320–5. doi: 10.2967/jnumed.116.178996

227. Fujita M, Kobayashi M, Ikawa M, Gunn RN, Rabiner EA, Owen DR, et al. Comparison of four 11 C-labeled PET ligands to quantify translocator protein 18 kDa (TSPO) in human brain: (R)-PK11195, PBR28, DPA-713, and ER176-based on recent publications that measured specific-to-non-displaceable ratios. *EJNMMI Res.* (2017) 7:84. doi: 10.1186/s13550-017-0334-8

228. Zanotti-Fregonara P, Pascual B, Veronese M, Yu M, Beers D, Appel SH, et al. Head-to-head comparison of 11 C-PBR28 and 11 C-ER176 for quantification of the translocator protein in the human brain. *Eur J Nucl Med Mol Imaging.* (2019) 47:1822–9. doi: 10.1007/s00259-019-04349-w

229. Siméon FG, Lee JH, Morse CL, Stukes I, Zoghbi SS, Manly LS, et al. Synthesis and screening in mice of fluorine-containing PET radioligands for TSPO: discovery of a promising 18 F-labeled ligand. *J Med Chem.* (2021) 64:16731–45. doi: 10.1021/acs.jmedchem.1c01562

230. Lee J-H, Simeon FG, Liow J-S, Morse CL, Gladding RL, Montero Santamaria JA, et al. *In vivo* evaluation of six analogs of 11 C-ER176 as candidate 18 F-labeled radioligands for translocator protein 18 kDa (TSPO). *J Nucl Med.* (2022). doi: 10.2967/jnumed.121.263168. [Epub ahead of print].

231. Ramakrishnan NK, Hird M, Thompson S, Williamson DJ, Qiao L, Owen DR, et al. Preclinical evaluation of (S)-[18 F]GE387, a novel 18-kDa translocator protein (TSPO) PET radioligand with low binding sensitivity to human polymorphism rs6971. *Eur J Nucl Med Mol Imaging.* (2021) 49:125–36. doi: 10.1007/s00259-021-05495-w

232. MacAskill MG, Wimberley C, Morgan TEF, Alcaide-Corral CJ, Newby DE, Lucatelli C, et al. Modelling [18 F]LW223 PET data using simplified

imaging protocols for quantification of TSPO expression in the rat heart and brain. *Eur J Nucl Med Mol Imaging.* (2021) 49:137–45. doi: 10.1007/s00259-021-05482-1

233. MacAskill MG, Stadulyte A, Williams L, Morgan TEF, Sloan NL, Alcaide-Corral CJ, et al. Quantification of macrophage-driven inflammation during myocardial infarction with 18 F-LW223, a novel TSPO radiotracer with binding independent of the rs6971 human polymorphism. *J Nucl Med.* (2021) 62:536–44. doi: 10.2967/jnumed.120.243600

234. Lee SH, Denora N, Laquintana V, Mangiatordi GF, Lopedota A, Lopalco A, et al. Radiosynthesis and characterization of [18 F]BS224: a next-generation TSPO PET ligand insensitive to the rs6971 polymorphism. *Eur J Nucl Med Mol Imaging.* (2021) 49:110–24. doi: 10.1007/s00259-021-05617-4

235. Locke LW, Mayo MW, Yoo AD, Williams MB, Berr SS. PET Imaging of tumor associated macrophages using mannose coated 64Cu liposomes. *Biomaterials.* (2012) 33:7785–93. doi: 10.1016/j.biomaterials.2012.07.022

236. Lee SP, Im HJ, Kang S, Chung SJ, Cho YS, Kang H, et al. Noninvasive imaging of myocardial inflammation in myocarditis using 68 Ga-tagged mannosylated human serum albumin positron emission tomography. *Theranostics.* (2017) 7:413–24. doi: 10.7150/thno.15712

237. Eo JS, Kim HK, Kim S, Lee YS, Jeong JM, Choi YH. Gallium-68 neomannosylated human serum albumin-based PET/CT lymphoscintigraphy for sentinel lymph node mapping in non-small cell lung cancer. *Ann Surg Oncol.* (2015) 22:636–41. doi: 10.1245/s10434-014-3986-x

238. Choi JY, Jeong JM, Yoo BC, Kim K, Kim Y, Yang BY, et al. Development of 68Ga-labeled mannosylated human serum albumin (MSA) as a lymph node imaging agent for positron emission tomography. *Nucl Med Biol.* (2011) 38:371–9. doi: 10.1016/j.nucmedbio.2010.09.010

239. Kim EJ, Kim S, Seo HS, Lee YJ, Eo JS, Jeong JM, et al. Novel PET Imaging of atherosclerosis with 68Ga-labeled NOTA-neomannosylated human serum albumin. *J Nucl Med.* (2016) 57:1792–7. doi: 10.2967/jnumed.116.172650

240. Fukuda H, Matsuzawa T, Abe Y, Endo S, Yamada K, Kubota K, et al. Experimental study for cancer diagnosis with positron-labeled fluorinated glucose analogs: [18F]-2-fluoro-2-deoxy-D-mannose: a new tracer for cancer detection. *Eur J Nucl Med.* (1982) 7:294–7. doi: 10.1007/BF00253423

241. Wienhard K, Pawlik G, Nebeling B, Rudolf J, Fink G, Hamacher K, et al. Estimation of local cerebral glucose utilization by positron emission tomography: comparison of [18F]2-fluoro-2-deoxy-D-glucose and [18F]2-fluoro-2-deoxy-D-mannose in patients with focal brain lesions. *J Cereb Blood Flow Metab.* (1991) 11:485–91. doi: 10.1038/jcbfm.1991.92

242. Qin Z, Hoh CK, Olson ES, Jahromi AH, Hall DJ, Barback C V, et al. Molecular Imaging of the Glomerulus via Mesangial Cell Uptake of Radiolabeled Tilmanocept. *J Nucl Med.* (2019) 60:1325–32. doi: 10.2967/jnumed.118.223727

243. Blykers A, Schoonooghe S, Xavier C, D'Hoe K, Laoui D, D'Huyvetter M, et al. PET imaging of macrophage mannose receptor-expressing macrophages in tumor stroma using 18F-radiolabeled camelid single-domain antibody fragments. *J Nucl Med.* (2015) 56:1265–71. doi: 10.2967/jnumed.115.156828

244. Senders ML, Hernot S, Carlucci G, van de Voort JC, Fay F, Calcagno C, et al. Nanobody-facilitated multiparametric PET/MRI phenotyping of atherosclerosis. *JACC Cardiovasc Imaging.* (2019) 12:2015. doi: 10.1016/j.jcmg.2018.07.027

245. Xavier C, Blykers A, Laoui D, Bolli E, Vaneyken I, Bridoux J, et al. Clinical translation of [68 Ga]Ga-NOTA-anti-MMR-sdAb for PET/CT imaging of protumorigenic macrophages. *Mol imaging Biol.* (2019) 21:898–906. doi: 10.1007/s11307-018-01302-5

246. Varasteh Z, Mohanta S, Li Y, López Armbruster N, Braeuer M, Nekolla SG, et al. Targeting mannose receptor expression on macrophages in atherosclerotic plaques of apolipoprotein E-knockout mice using 68 Ga-NOTA-anti-MMR nanobody: non-invasive imaging of atherosclerotic plaques. *EJNMMI Res.* (2019) 9:5. doi: 10.1186/s13550-019-0474-0

247. Bettio A, Honer M, Müller C, Brühlmeier M, Müller U, Schibli R, et al. Synthesis and preclinical evaluation of a folic acid derivative labeled with 18F for PET imaging of folate receptor-positive tumors. *J Nucl Med.* (2006) 47:1153–60.

248. Ross TL, Honer M, Lam PYH, Mindt TL, Groehn V, Schibli R, et al. Fluorine-18 click radiosynthesis and preclinical evaluation of a new 18F-labeled folic acid derivative. *Bioconjug Chem.* (2008) 19:2462–70. doi: 10.1021/bc800356r

249. Fani M, Wang X, Nicolas G, Medina C, Raynal I, Port M, et al. Development of new folate-based PET radiotracers: preclinical evaluation of ^{68}Ga-DOTA-folate conjugates. *Eur J Nucl Med Mol Imaging.* (2011) 38:108–19. doi: 10.1007/s00259-010-1597-8

250. Ross TL, Honer M, Müller C, Groehn V, Schibli R, Ametamey SM, et al. new 18F-labeled folic acid derivative with improved properties for the PET imaging of folate receptor-positive tumors. *J Nucl Med.* (2010) 51:1756–62. doi: 10.2967/jnumed.110.079756

251. Jammaz IA, Al-Otaibi B, Amer S, Okarvi SM. Rapid synthesis and in vitro and in vivo evaluation of folic acid derivatives labeled with fluorine-18 for PET imaging of folate receptor-positive tumors. *Nucl Med Biol.* (2011) 38:1019–28. doi: 10.1016/j.nucmedbio.2011.03.004

252. Fischer CR, Müller C, Reber J, Müller A, Krämer SD, Ametamey SM, et al. [18F]fluoro-deoxy-glucose folate: a novel PET radiotracer with improved *in vivo* properties for folate receptor targeting. *Bioconjug Chem.* (2012) 23:805–13. doi: 10.1021/bc200660z

253. Al Jammaz I, Al-Otaibi B, Amer S, Al-Hokbany N, Okarvi S. Novel synthesis and preclinical evaluation of folic acid derivatives labeled with (18)F-[FDG] for PET imaging of folate receptor-positive tumors. *Nucl Med Biol.* (2012) 39:864–70. doi: 10.1016/j.nucmedbio.2012.02.005

254. Fischer CR, Groehn V, Reber J, Schibli R, Ametamey SM, Müller C. Improved PET imaging of tumors in mice using a novel (18) F-folate conjugate with an albumin-binding entity. *Mol imaging Biol.* (2013) 15:649–54. doi: 10.1007/s11307-013-0651-x

255. Fani M, Tamma ML, Nicolas GP, Lasri E, Medina C, Raynal I, et al. *In vivo* imaging of folate receptor positive tumor xenografts using novel 68Ga-NODAGA-folate conjugates. *Mol Pharm.* (2012) 9:1136–45. doi: 10.1021/mp200418f

256. Kühle B, Müller C, Ross TL. A novel (68)Ga-labeled pteroic acid-based pet tracer for tumor imaging via the folate receptor. *Recent Results Cancer Res.* (2013) 194:257–67. doi: 10.1007/978-3-642-27994-2_13

257. Betzel T, Müller C, Groehn V, Müller A, Reber J, Fischer CR, et al. Radiosynthesis and preclinical evaluation of 3'-Aza-2'-[(18)F]fluorofolic acid: a novel PET radiotracer for folate receptor targeting. *Bioconjug Chem.* (2013) 24:205–14. doi: 10.1021/bc300483a

258. Gnesin S, Müller J, Burger IA, Meisel A, Siano M, Früh M, et al. Radiation dosimetry of 18 F-AzaFol: a first in-human use of a folate receptor PET tracer. *EJNMMI Res.* (2020) 10:32. doi: 10.1186/s13550-020-00624-2

259. Schniering J, Benešová M, Brunner M, Haller S, Cohrs S, Frauenfelder T, et al. 18 F-AzaFol for detection of folate receptor-β positive macrophages in experimental interstitial lung disease-a proof-of-concept study. *Front Immunol.* (2019) 10:2724. doi: 10.3389/fimmu.2019.02724

260. Gent YYJ, Weijers K, Molthoff CFM, Windhorst AD, Huisman MC, Smith DEC, et al. Evaluation of the novel folate receptor ligand [18F]fluoro-PEG-folate for macrophage targeting in a rat model of arthritis. *Arthritis Res Ther.* (2013) 15:R37. doi: 10.1186/ar4191

261. Chandrupatla DMSH, Molthoff CFM, Ritsema WIGR, Vos R, Elshof E, Matsuyama T, et al. Prophylactic and therapeutic activity of alkaline phosphatase in arthritic rats: single-agent effects of alkaline phosphatase and synergistic effects in combination with methotrexate. *Transl Res.* (2018) 199:24–38. doi: 10.1016/j.trsl.2018.04.001

262. Chandrupatla DMSH, Jansen G, Mantel E, Low PS, Matsuyama T, Musters RP, et al. Imaging and methotrexate response monitoring of systemic inflammation in arthritic rats employing the macrophage PET Tracer [18 F]Fluoro-PEG-Folate. *Contrast Media Mol Imaging.* (2018) 2018:8092781. doi: 10.1155/2018/8092781

263. Verweij NJF, Yaqub M, Bruijnen STG, Pieplenbosch S, ter Wee MM, Jansen G, et al. First in man study of [18 F]fluoro-PEG-folate PET: a novel macrophage imaging technique to visualize rheumatoid arthritis. *Sci Rep.* (2020) 10:1047. doi: 10.1038/s41598-020-57841-x

264. Kularatne SA, Bélanger MJ, Meng X, Connolly BM, Vanko A, Suresch DL, et al. Comparative analysis of folate derived PET imaging agents with [(18)F]-2-fluoro-2-deoxy-d-glucose using a rodent inflammatory paw model. *Mol Pharm.* (2013) 10:3103–11. doi: 10.1021/mp4001684

265. Aljammaz I, Al-Otaibi B, Al-Hokbany N, Amer S, Okarvi S. Development and pre-clinical evaluation of new 68Ga-NOTA-folate conjugates for PET imaging of folate receptor-positive tumors. *Anticancer Res.* (2014) 34:6547–56.

266. Brand C, Longo VA, Groaning M, Weber WA, Reiner T. Development of a new folate-derived Ga-68-based PET imaging agent. *Mol imaging Biol.* (2017) 19:754–61. doi: 10.1007/s11307-017-1049-y

267. Boss SD, Betzel T, Müller C, Fischer CR, Haller S, Reber J, et al. Comparative studies of three pairs of α- and γ-conjugated folic acid derivatives labeled with fluorine-18. *Bioconjug Chem.* (2016) 27:74–86. doi: 10.1021/acs.bioconjchem.5b00644

268. Chen Q, Meng X, McQuade P, Rubins D, Lin SA, Zeng Z, et al. Synthesis and preclinical evaluation of folate-NOTA-Al(18)F for PET imaging of folate-receptor-positive tumors. *Mol Pharm.* (2016) 13:1520–7. doi: 10.1021/acs.molpharmaceut.5b00989

269. Farkas R, Siwowska K, Ametamey SM, Schibli R, Van Der Meulen NP, Müller C. (64)Cu- and (68)Ga-based PET imaging of folate receptor-positive tumors: development and evaluation of an albumin-binding NODAGA-folate. *Mol Pharm.* (2016) 13:1979–87. doi: 10.1021/acs.molpharmaceut.6b00143

270. Zhang X, Yu Q, He Y, Zhang C, Zhu H, Yang Z, et al. Synthesis and biological evaluation of (68) Ga-labeled Pteroyl-Lys conjugates for folate receptor-targeted tumor imaging. *J Labelled Comp Radiopharm.* (2016) 59:346–53. doi: 10.1002/jlcr.3410

271. Jain A, Mathur A, Pandey U, Bhatt J, Mukherjee A, Ram R, et al. Synthesis and evaluation of a (68)Ga labeled folic acid derivative for targeting folate receptors. *Appl Radiat Isot.* (2016) 116:77–84. doi: 10.1016/j.apradiso.2016.07.024

272. Li N, Yu Z, Pham TT, Blower PJ, Yan R, A. generic 89 Zr labeling method to quantify the *in vivo* pharmacokinetics of liposomal nanoparticles with positron emission tomography. *Int J Nanomed.* (2017) 12:3281–94. doi: 10.2147/IJN.S134379

273. Choi PS, Lee JY, Park JH, Kim SW. Synthesis and evaluation of 68 Ga-HBED-CC-EDBE-folate for positron-emission tomography imaging of overexpressed folate receptors on CT26 tumor cells. *J Labelled Comp Radiopharm.* (2018) 61:4–10. doi: 10.1002/jlcr.3563

274. Chen Q, Meng X, McQuade P, Rubins D, Lin SA, Zeng Z, et al. Folate-PEG-NOTA-Al 18 F: a new folate based radiotracer for PET imaging of folate receptor-positive tumors. *Mol Pharm.* (2017) 14:4353–61. doi: 10.1021/acs.molpharmaceut.7b00415

275. Ma W, Fu F, Zhu J, Huang R, Zhu Y, Liu Z, et al. 64 Cu-Labeled multifunctional dendrimers for targeted tumor PET imaging. *Nanoscale.* (2018) 10:6113–24. doi: 10.1039/C7NR09269E

276. Kettenbach K, Reffert LM, Schieferstein H, Pektor S, Eckert R, Miederer M, et al. Comparison study of two differently clicked 18 F-folates-lipophilicity plays a key role. *Pharmaceuticals.* (2018) 11:30. doi: 10.3390/ph110 10030

277. Silvola JMU, Li XG, Virta J, Marjamäki P, Liljenbäck H, Hytönen JP, et al. Aluminum fluoride-18 labeled folate enables in vivo detection of atherosclerotic plaque inflammation by positron emission tomography. *Sci Rep.* (2018) 8:9720. doi: 10.1038/s41598-018-27618-4

278. Jahandideh A, Uotila S, Ståhle M, Virta J, Li XG, Kytö V, et al. Folate receptor β-targeted PET imaging of macrophages in autoimmune myocarditis. *J Nucl Med.* (2020) 61:1643–9. doi: 10.2967/jnumed.119.241356

279. Körhegyi Z, Rózsa D, Hajdu I, Bodnár M, Kertész I, Kerekes K, et al. Synthesis of 68 Ga-labeled biopolymer-based nanoparticle imaging agents for positron-emission tomography. *Anticancer Res.* (2019) 39:2415–27. doi: 10.21873/anticanres.13359

280. Radford LL, Fernandez S, Beacham R, Sayed R El, Farkas R, Benešová M, et al. New 55 co-labeled albumin-binding folate derivatives as potential PET agents for folate receptor imaging. *Pharmaceuticals.* (2019) 12:166. doi: 10.3390/ph12040166

281. Larenkov A, Rakhimov M, Lunyova K, Klementyeva O, Maruk A, Machulkin A. Pharmacokinetic properties of 68 Ga-labelled folic acid conjugates: improvement using HEHE Tag. *Molecules.* (2020) 25:2712. doi: 10.3390/molecules25112712

282. Kim GG, Lee JY, Choi PS, Kim SW, Park JH. Tumor targeting effect of triphenylphosphonium cations and folic acid coated with Zr-89-labeled silica nanoparticles. *Molecules.* (2020) 25:2922. doi: 10.3390/molecules251 22922

283. Moisio O, Palani S, Virta J, Elo P, Liljenbäck H, Tolvanen T, et al. Radiosynthesis and preclinical evaluation of [68 Ga]Ga-NOTA-folate for PET imaging of folate receptor β-positive macrophages. *Sci Rep.* (2020) 10:13593. doi: 10.1038/s41598-020-70394-3

284. Kim GG, Jang HM, Park SB, So JS, Kim SW. Synthesis of Zr-89-labeled folic acid-conjugated silica (SiO 2) microwire as a tumor diagnostics carrier for positron emission tomography. *Materials.* (2021) 14:3226. doi: 10.3390/ma14123226

285. Taddio MF, Castro Jaramillo CA, Runge P, Blanc A, Keller C, Talip Z, et al. *In vivo* imaging of local inflammation: monitoring LPS-induced CD80/CD86 upregulation by PET. *Mol imaging Biol.* (2021) 23:196–207. doi: 10.1007/s11307-020-01543-3

286. Zhang J, McCarthy TJ, Moore WM, Currie MG, Welch MJ. Synthesis and evaluation of two positron-labeled nitric oxide synthase inhibitors, S-[11C]methylisothiourea and S-(2-[18F]fluoroethyl)isothiourea, as potential positron emission tomography tracers. *J Med Chem.* (1996) 39:5110–8. doi: 10.1021/jm960481q

287. Tian H, Lee Z. Radiosynthesis of 8-Fluoro-3-(4-[18F]Fluorophenyl)-3,4-Dihydro-1-Isoquinolinamine ([18F]FFDI), a potential PET radiotracer for the inducible nitric oxide synthase. *Curr Radiopharm.* (2008) 1:49–53. doi: 10.2174/1874471010801020049

288. Zhou D, Lee H, Rothfuss JM, Chen DL, Ponde DE, Welch MJ, et al. Design and synthesis of 2-amino-4-methylpyridine analogues as inhibitors for inducible nitric oxide synthase and *in vivo* evaluation of [18F]6-(2-fluoropropyl)-4-methyl-pyridin-2-amine as a potential PET tracer for inducible nitric oxide synthase. *J Med Chem.* (2009) 52:2443–53. doi: 10.1021/jm801556h

289. Herrero P, Laforest R, Shoghi K, Zhou D, Ewald G, Pfeifer J, et al. Feasibility and dosimetry studies for 18F-NOS as a potential PET radiopharmaceutical for inducible nitric oxide synthase in humans. *J Nucl Med.* (2012) 53:994–1001. doi: 10.2967/jnumed.111.088518

290. Huang HJ, Isakow W, Byers DE, Engle JT, Griffin EA, Kemp D, et al. Imaging pulmonary inducible nitric oxide synthase expression with PET. *J Nucl Med.* (2015) 56:76–81. doi: 10.2967/jnumed.114.146381

291. Yeh SHH, Huang WS, Chiu CH, Chen CL, Chen HT, Chi DY, et al. Automated Synthesis and Initial Evaluation of (4'-Amino-5',8'-difluoro-1'H-spiro[piperidine-4,2'-quinazolin]-1-yl)(4-[18F]fluorophenyl)methanone for PET/MR Imaging of Inducible Nitric Oxide Synthase. *Mol Imaging.* (2021) 2021:9996125. doi: 10.1155/2021/9996125

292. Liu Y, Gunsten SP, Sultan DH, Luehmann HP, Zhao Y, Blackwell TS, et al. PET-based Imaging of Chemokine Receptor 2 in experimental and disease-related lung inflammation. *Radiology.* (2017) 283:758–68. doi: 10.1148/radiol.2016161409

293. Liu Y, Li W, Luehmann HP, Zhao Y, Detering L, Sultan DH, et al. Noninvasive imaging of CCR2 + cells in ischemia-reperfusion injury after lung transplantation. *Am J Transplant.* (2016) 16:3016–23. doi: 10.1111/ajt.13907

294. Li W, Luehmann HP, Hsiao HM, Tanaka S, Higashikubo R, Gauthier JM, et al. Visualization of monocytic cells in regressing atherosclerotic plaques by intravital 2-photon and positron emission tomography-based imaging-brief report. *Arterioscler Thromb Vasc Biol.* (2018) 38:1030–6. doi: 10.1161/ATVBAHA.117.310517

295. Dobrucki LW, Sinusas AJ. Targeted imaging of abdominal aortic aneurysm: biology over structure. *Circ Cardiovasc Imaging.* (2020) 13:e010495. doi: 10.1161/CIRCIMAGING.120.010495

296. English SJ, Sastriques SE, Detering L, Sultan D, Luehmann H, Arif B, et al. CCR2 positron emission tomography for the assessment of abdominal aortic aneurysm inflammation and rupture prediction. *Circ Cardiovasc Imaging.* (2020) 13:e009889. doi: 10.1161/CIRCIMAGING.119.009889

297. Heo GS, Kopecky B, Sultan D, Ou M, Feng G, Bajpai G, et al. Molecular imaging visualizes recruitment of inflammatory monocytes and macrophages to the injured heart. *Circ Res.* (2019) 124:881–90. doi: 10.1161/CIRCRESAHA.118.314030

298. Brody SL, Gunsten SP, Luehmann HP, Sultan DH, Hoelscher M, Heo GS, et al. Chemokine receptor 2-targeted molecular imaging in pulmonary fibrosis. A clinical trial. *Am J Respir Crit Care Med.* (2021) 203:78–89. doi: 10.1164/rccm.202004-1132OC

299. Heo GS, Bajpai G, Li W, Luehmann HP, Sultan DH, Dun H, et al. Targeted PET imaging of chemokine receptor 2-positive monocytes and macrophages in the injured heart. *J Nucl Med.* (2021) 62:111–4. doi: 10.2967/jnumed.120.244673

300. Sultan D, Li W, Detering L, Heo GS, Luehmann HP, Kreisel D, Liu Y. Assessment of ultrasmall nanocluster for early and accurate detection of atherosclerosis using positron emission tomography/computed tomography. *Nanomedicine.* (2021) 36:102416. doi: 10.1016/j.nano.2021.102416

301. Zhang X, Detering L, Sultan D, Luehmann H, Li L, Heo GS, et al. CC Chemokine receptor 2-targeting copper nanoparticles for positron emission tomography-guided delivery of gemcitabine for pancreatic ductal adenocarcinoma. *ACS Nano.* (2021) 15:1186–98. doi: 10.1021/acsnano.0c08185

302. Wagner S, de Moura Gatti F, Silva DG, Ortiz Zacarias N V, Zweemer AJM, Hermann S, et al. Development of the first potential nonpeptidic positron emission tomography tracer for the imaging of CCR2 receptors. *ChemMedChem.* (2021) 16:640–5. doi: 10.1002/cmdc.202000728

303. Gao M, Wang M, Meyer JA, Peters JS, Zarrinmayeh H, Territo PR, et al. Synthesis and preliminary biological evaluation of [11 C]methyl (2-amino-5-(benzylthio)thiazolo[4,5-d]pyrimidin-7-yl)-d-leucinate for the fractalkine receptor (CX 3 CR1). *Bioorg Med Chem Lett.* (2017) 27:2727–30. doi: 10.1016/j.bmcl.2017.04.052

304. Jayson GC, Zweit J, Jackson A, Mulatero C, Julyan P, Ranson M, et al. Molecular imaging and biological evaluation of HuMV833 anti-VEGF antibody: implications for trial design of antiangiogenic antibodies. *J Natl Cancer Inst.* (2002) 94:1484–93. doi: 10.1093/jnci/94.19.1484

305. Collingridge DR, Carroll VA, Glaser M, Aboagye EO, Osman S, Hutchinson OC, et al. The development of [(124)I]iodinated-VG76e: a novel tracer for imaging vascular endothelial growth factor in vivo using positron emission tomography. *Cancer Res.* (2002) 62:5912–9.

306. Nagengast WB, De Vries EG, Hospers GA, Mulder NH, De Jong JR, Hollema H, et al. Lub-de Hooge MN. *In vivo* VEGF imaging with radiolabeled bevacizumab in a human ovarian tumor xenograft. *J Nucl Med.* (2007) 48:1313–9. doi: 10.2967/jnumed.107.041301

307. Nagengast WB, de Korte MA, Oude Munnink TH, Timmer-Bosscha H, den Dunnen WF, Hollema H, et al. 89Zr-bevacizumab PET of early antiangiogenic tumor response to treatment with HSP90 inhibitor NVP-AUY922. *J Nucl Med.* (2010) 51:761–7. doi: 10.2967/jnumed.109.071043

308. Van Es SC, Brouwers AH, Mahesh SVK, Leliveld-Kors AM, De Jong IJ, Lub-De Hooge MN, et al. 89 Zr-Bevacizumab PET: potential early indicator of everolimus efficacy in patients with metastatic renal cell carcinoma. *J Nucl Med.* (2017) 58:905–10. doi: 10.2967/jnumed.116.183475

309. Golestani R, Zeebregts CJ, Terwissscha van Scheltinga AGT, Lub-de Hooge MN, van Dam GM, Glaudemans AWJM, et al. Feasibility of vascular endothelial growth factor imaging in human atherosclerotic plaque using (89)Zr-bevacizumab positron emission tomography. *Mol Imaging.* (2013) 12:235–43. doi: 10.2310/7290.2012.00034

310. Van Der Bilt ARM, Terwissscha Van Scheltinga AGT, Timmer-Bosscha H, Schröder CP, Pot L, Kosterink JGW, et al. Measurement of tumor VEGF-A levels with 89Zr-bevacizumab PET as an early biomarker for the antiangiogenic effect of everolimus treatment in an ovarian cancer xenograft model. *Clin Cancer Res.* (2012) 18:6306–14. doi: 10.1158/1078-0432.CCR-12-0406

311. Gaykema SBM, Brouwers AH, Hooge MNL De, Pleijhuis RG, Timmer-Bosscha H, Pot L, et al. 89Zr-bevacizumab PET imaging in primary breast cancer. *J Nucl Med.* (2013) 54:1014–8. doi: 10.2967/jnumed.112.117218

312. Van Asselt SJ, Oosting SF, Brouwers AH, Bongaerts AHH, De Jong JR, Lub-de Hooge MN, et al. Everolimus reduces (89)Zr-bevacizumab tumor uptake in patients with neuroendocrine. *Tumors J Nucl Med.* (2014) 55:1087–92. doi: 10.2967/jnumed.113.129056

313. Van Scheltinga AG, Berghuis P, Nienhuis HH, Timmer-Bosscha H, Pot L, Gaykema SB, et al. Visualising dual downregulation of insulin-like growth factor receptor-1 and vascular endothelial growth factor-A by heat shock protein 90 inhibition effect in triple negative breast cancer. *Eur J Cancer.* (2014) 50:2508–16. doi: 10.1016/j.ejca.2014.06.008

314. Oosting SF, Brouwers AH, Van Es SC, Nagengast WB, Munnink THO, Lub-De Hooge MN, et al. 89Zr-bevacizumab PET visualizes heterogeneous tracer accumulation in tumor lesions of renal cell carcinoma patients and differential effects of antiangiogenic treatment. *J Nucl Med.* (2015) 56:63–9. doi: 10.2967/jnumed.114.144840

315. Oosting SF, Van Asselt SJ, Brouwers AH, Bongaerts AHH, Steinberg JDJ, De Jong JR, et al. 89Zr-Bevacizumab PET visualizes disease manifestations in

316. Jansen MHA, Lagerweij T, Sewing ACP, Vugts DJ, Van Vuurden DG, Molthoff CFM, et al. Bevacizumab targeting diffuse intrinsic pontine glioma: results of 89Zr-bevacizumab PET imaging in brain tumor models. *Mol Cancer Ther.* (2016) 15:2166–74. doi: 10.1158/1535-7163.MCT-15-0558

317. Jansen MH, Van Zanten SEMV, Van Vuurden DG, Huisman MC, Vugts DJ, Hoekstra OS, et al. Molecular drug imaging: 89 Zr-Bevacizumab PET in children with diffuse intrinsic pontine glioma. *J Nucl Med.* (2017) 58:711–6. doi: 10.2967/jnumed.116.180216

318. Paudyal B, Paudyal P, Oriuchi N, Hanaoka H, Tominaga H, Endo K. Positron emission tomography imaging and biodistribution of vascular endothelial growth factor with 64Cu-labeled bevacizumab in colorectal cancer xenografts. *Cancer Sci.* (2011) 102:117–21. doi: 10.1111/j.1349-7006.2010.01763.x

319. Nagengast WB, Lub-de Hooge MN, Oosting SF, Den Dunnen WFA, Warnders FJ, Brouwers AH, et al. VEGF-PET imaging is a noninvasive biomarker showing differential changes in the tumor during sunitinib treatment. *Cancer Res.* (2011) 71:143–53. doi: 10.1158/0008-5472.CAN-10-1088

320. Zhang Y, Hong H, Engle JW, Yang Y, Barnhart TE, Cai W. Positron emission tomography and near-infrared fluorescence imaging of vascular endothelial growth factor with dual-labeled bevacizumab. *Am J Nucl Med Mol Imaging.* (2012) 2:1–13.

321. Christoforidis JB, Williams MM, Kothandaraman S, Kumar K, Epitropoulos FJ, Knopp M V. Pharmacokinetic properties of intravitreal I-124-aflibercept in a rabbit model using PET/CT. *Curr Eye Res.* (2012) 37:1171–4. doi: 10.3109/02713683.2012.727521

322. Chang AJ, Sohn R, Lu ZH, Arbeit JM, Lapi SE. Detection of rapalog-mediated therapeutic response in renal cancer xenografts using ^{64}Cu-bevacizumab immunoPET. *PLoS ONE.* (2013) 8:58949. doi: 10.1371/journal.pone.0058949

323. Marquez B V, Ikotun OF, Parry JJ, Rogers BE, Meares CF, Lapi SE. Development of a radiolabeled irreversible peptide ligand for PET imaging of vascular endothelial growth factor. *J Nucl Med.* (2014) 55:1029–34. doi: 10.2967/jnumed.113.130898

324. Owen DR, Yeo AJ, Gunn RN, Song K, Wadsworth G, Lewis A, et al. An 18-kDa translocator protein (TSPO) polymorphism explains differences in binding affinity of the PET radioligand PBR28. *J Cereb Blood Flow Metab.* (2012) 32:1–5. doi: 10.1038/jcbfm.2011.147

325. Owen DRJ, Gunn RN, Rabiner EA, Bennacef I, Fujita M, Kreisl WC, et al. Mixed-affinity binding in humans with 18-kDa translocator protein ligands. *J Nucl Med.* (2011) 52:24–32. doi: 10.2967/jnumed.110.079459

326. Turkheimer FE, Rizzo G, Bloomfield PS, Howes O, Zanotti-Fregonara P, Bertoldo A, et al. The methodology of TSPO imaging with positron emission tomography. *Biochem Soc Trans.* (2015) 43:586–92. doi: 10.1042/BST20150058

327. Schollhammer R, Lepreux S, Barthe N, Vimont D, Rullier A, Sibon I, et al. *In vitro* and pilot *in vivo* imaging of 18 kDa translocator protein (TSPO) in inflammatory vascular disease. *EJNMMI Res.* (2021) 11:45. doi: 10.1186/s13550-021-00786-7

328. Tahara N, Mukherjee J, De Haas HJ, Petrov AD, Tawakol A, Haider N, et al. 2-deoxy-2-[18F]fluoro-D-mannose positron emission tomography imaging in atherosclerosis. *Nat Med.* (2014) 20:215–9. doi: 10.1038/nm.3437

329. Mathias CJ, Wang S, Lee RJ, Waters DJ, Low PS, Green MA. Tumor-Selective Radiopharmaceutical targeting via receptor-mediated endocytosis of gallium-67-deferoxamine-folate. *J Nucl Med.* (1996) 37:1003–8.

330. Mathias CJ, Lewis MR, Reichert DE, Laforest R, Sharp TL, Lewis JS, et al. Preparation of 66Ga- and 68Ga-labeled Ga(III)-deferoxamine-folate as potential folate-receptor-targeted PET radiopharmaceuticals. *Nucl Med Biol.* (2003) 30:725–31. doi: 10.1016/S0969-8051(03)00080-5

331. Müller C, Zhernosekov K, Köster U, Johnston K, Dorrer H, Hohn A, et al. unique matched quadruplet of terbium radioisotopes for PET and SPECT and for α- and β- radionuclide therapy: an *in vivo* proof-of-concept study with a new receptor-targeted folate derivative. *J Nucl Med.* (2012) 53:1951–9. doi: 10.2967/jnumed.112.107540

332. AlJammaz I, Al-Otaibi B, Al-Rumayan F, Al-Yanbawi S, Amer S, Okarvi SM. Development and preclinical evaluation of new (124)I-folate conjugates

patients with von Hippel-Lindau Disease. *J Nucl Med.* (2016) 57:1244–50. doi: 10.2967/jnumed.115.167643

for PET imaging of folate receptor-positive tumors. *Nucl Med Biol.* (2014) 41:457–63. doi: 10.1016/j.nucmedbio.2014.03.013

333. Zhou M, Song S, Zhao J, Tian M, Li C. Theranostic CuS nanoparticles targeting folate receptors for PET image-guided photothermal therapy. *J Mater Chem B.* (2015) 3:8939–48. doi: 10.1039/C5TB01866H

334. Van Der Geest KSM, Wolfe K, Borg F, Sebastian A, Kayani A, Tomelleri A, et al. Ultrasonographic Halo Score in giant cell arteritis: association with intimal hyperplasia and ischaemic sight loss. *Rheumatology.* (2021) 60:4361–6. doi: 10.1093/rheumatology/keaa806

335. Langford CA, Cuthbertson D, Ytterberg SR, Khalidi N, Monach PA, Carette S, et al. A randomized, double-blind trial of abatacept (CTLA-4Ig) for the treatment of giant cell arteritis. *Arthritis Rheumatol.* (2017) 69:837–45. doi: 10.1002/art.40044

336. Toussirot E, Michaud M, Wendling D, Devauchelle V. Abatacept as adjunctive therapy in refractory polymyalgia rheumatica. *J Rheumatol.* (2021) 48:1888–9. doi: 10.3899/jrheum.210455

337. Goodfellow N, Morlet J, Singh S, Sabokbar A, Hutchings A, Sharma V, et al. Is vascular endothelial growth factor a useful biomarker in giant cell arteritis? *RMD Open.* (2017) 3:e000353. doi: 10.1136/rmdopen-2016-000353

338. Van Der Geest KSM, Abdulahad WH, Chalan P, Rutgers A, Horst G, Huitema MG, et al. Disturbed B cell homeostasis in newly diagnosed giant cell arteritis and polymyalgia rheumatica. *Arthritis Rheumatol.* (2014) 66:1927–38. doi: 10.1002/art.38625

339. Olafsen T, Betting D, Kenanova VE, Salazar FB, Clarke P, Said J, et al. Recombinant anti-CD20 antibody fragments for small-animal PET imaging of B-cell lymphomas. *J Nucl Med.* (2009) 50:1500–8. doi: 10.2967/jnumed.108.060426

340. Olafsen T, Sirk SJ, Betting DJ, Kenanova VE, Bauer KB, Ladno W, et al. ImmunoPET imaging of B-cell lymphoma using 124I-anti-CD20 scFv dimers (diabodies). *Protein Eng Des Sel.* (2010) 23:243–9. doi: 10.1093/protein/gzp081

341. Tran L, Huitema ADR, Van Rijswijk MH, Dinant HJ, Baars JW, Beijnen JH, et al. CD20 antigen imaging with [124]I-rituximab PET/CT in patients with rheumatoid arthritis. *Hum Antibodies.* (2011) 20:29–35. doi: 10.3233/HAB-2011-0239

342. Tran L, Vogel W V, Sinaasappel M, Muller S, Baars JW, Van Rijswijk M, et al. The pharmacokinetics of [124]I-rituximab in patients with rheumatoid arthritis. *Hum Antibodies.* (2011) 20:7–14. doi: 10.3233/HAB-2011-0237

343. Natarajan A, Habte F, Liu H, Sathirachinda A, Hu X, Cheng Z, et al. Evaluation of 89Zr-rituximab tracer by Cerenkov luminescence imaging and correlation with PET in a humanized transgenic mouse model to image NHL. *Mol Imaging Biol.* (2013) 15:468–75. doi: 10.1007/s11307-013-0624-0

344. Muylle K, Flamen P, Vugts DJ, Guiot T, Ghanem G, Meuleman N, et al. Tumour targeting and radiation dose of radioimmunotherapy with (90)Y-rituximab in CD20+ B-cell lymphoma as predicted by (89)Zr-rituximab immuno-PET: impact of preloading with unlabelled rituximab. *Eur J Nucl Med Mol Imaging.* (2015) 42:1304–14. doi: 10.1007/s00259-015-3025-6

345. de Jong A, Mous R, van Dongen GAMS, Hoekstra OS, Nievelstein RAJ, de Keizer B. (89) Zr-rituximab PET/CT to detect neurolymphomatosis. *Am J Hematol.* (2016) 91:649–50. doi: 10.1002/ajh.24328

346. Natarajan A, Gambhir SS. Radiation dosimetry study of [(89)Zr]rituximab tracer for clinical translation of B cell NHL imaging using positron emission tomography. *Mol Imaging Biol.* (2015) 17:539–47. doi: 10.1007/s11307-014-0810-8

347. Jauw YWS, Zijlstra JM, De Jong D, Vugts DJ, Zweegman S, Hoekstra OS, et al. Performance of 89Zr-labeled-rituximab-PET as an imaging biomarker to assess CD20 targeting: a pilot study in patients with relapsed/refractory diffuse large B cell lymphoma. *PLoS ONE.* (2017) 12:e0169828. doi: 10.1371/journal.pone.0169828

348. Bruijnen S, Tsang-A-Sjoe M, Raterman H, Ramwadhdoebe T, Vugts D, van Dongen G, et al. B-cell imaging with zirconium-89 labelled rituximab PET-CT at baseline is associated with therapeutic response 24weeks after initiation of rituximab treatment in rheumatoid arthritis patients. *Arthritis Res Ther.* (2016) 18:266. doi: 10.1186/s13075-016-1166-z

349. Natarajan A, Arksey N, Iagaru A, Chin FT, Gambhir SS. Validation of 64Cu-DOTA-rituximab injection preparation under good manufacturing practices: a PET tracer for imaging of B-cell non-Hodgkin lymphoma. *Mol Imaging.* (2015) 14:1–11. doi: 10.2310/7290.2014.00055

350. Natarajan A, Gowrishankar G, Nielsen CH, Wang S, Iagaru A, Goris ML, et al. Positron emission tomography of 64Cu-DOTA-Rituximab in a transgenic mouse model expressing human CD20 for clinical translation to image NHL. *Mol imaging Biol.* (2012) 14:608–16. doi: 10.1007/s11307-011-0537-8

351. Natarajan A, Hackel BJ, Gambhir SS. A novel engineered anti-CD20 tracer enables early time PET imaging in a humanized transgenic mouse model of B-cell non-Hodgkins lymphoma. *Clin Cancer Res.* (2013) 19:6820–9. doi: 10.1158/1078-0432.CCR-13-0626

352. Zettlitz KA, Tavaré R, Tsai WTK, Yamada RE, Ha NS, Collins J, et al. 18 F-labeled anti-human CD20 cys-diabody for same-day immunoPET in a model of aggressive B cell lymphoma in human CD20 transgenic mice. *Eur J Nucl Med Mol Imaging.* (2019) 46:489–500. doi: 10.1007/s00259-018-4214-x

353. Zettlitz KA, Tavaré R, Knowles SM, Steward KK, Timmerman JM, Wu AM. ImmunoPET of malignant and normal B cells with 89Zr- and 124I-labeled obinutuzumab antibody fragments reveals differential CD20 internalization *in vivo. Clin Cancer Res.* (2017) 23:7242. doi: 10.1158/1078-0432.CCR-17-0855

354. Bhatia A, Ell PJ, Edwards JCW. Anti-CD20 monoclonal antibody (rituximab) as an adjunct in the treatment of giant cell arteritis. *Ann Rheum Dis.* (2005) 64:1099–100. doi: 10.1136/ard.2005.036533

355. Li M, Younis MH, Zhang Y, Cai W, Lan X. Clinical summary of fibroblast activation protein inhibitor-based radiopharmaceuticals: cancer and beyond. *Eur J Nucl Med Mol Imaging.* (2022). doi: 10.1007/s00259-022-05706-y. [Epub ahead of print].

356. Meletta R, Herde AM, Chiotellis A, Isa M, Rancic Z, Borel N, et al. Evaluation of the radiolabeled boronic acid-based FAP inhibitor MIP-1232 for atherosclerotic plaque imaging. *Molecules.* (2015) 20:2081–99. doi: 10.3390/molecules20022081

357. Lindner T, Loktev A, Altmann A, Giesel F, Kratochwil C, Debus J, et al. Development of quinoline-based theranostic ligands for the targeting of fibroblast activation protein. *J Nucl Med.* (2018) 59:1415–22. doi: 10.2967/jnumed.118.210443

358. Moon ES, Elvas F, Vliegen G, De Lombaerde S, Vangestel C, De Bruycker S, et al. Targeting fibroblast activation protein (FAP): next generation PET radiotracers using squaramide coupled bifunctional DOTA and DATA 5m chelators. *EJNMMI Radiopharm Chem.* (2020) 5:19. doi: 10.1186/s41181-020-00102-z

359. Ballal S, Yadav MP, Moon ES, Kramer VS, Roesch F, Kumari S, et al. Biodistribution, pharmacokinetics, dosimetry of [68 Ga]Ga-DOTASAFAPi, and the head-to-head comparison with [18 F]F-FDG PET/CT in patients with various cancers. *Eur J Nucl Med Mol Imaging.* (2021) 48:1915–31. doi: 10.1007/s00259-020-05132-y

360. Wang G, Jin X, Zhu H, Wang S, Ding J, Zhang Y, et al. 68 Ga-NOTA-FAPI-04 PET/CT in a patient with primary gastric diffuse large B cell lymphoma: comparisons with [18 F] FDG PET/CT. *Eur J Nucl Med Mol Imaging.* (2021) 48:647–8. doi: 10.1007/s00259-020-04946-0

361. Loktev A, Lindner T, Burger EM, Altmann A, Giesel F, Kratochwil C, et al. Development of fibroblast activation protein-targeted radiotracers with improved tumor retention. *J Nucl Med.* (2019) 60:1421–9. doi: 10.2967/jnumed.118.224469

362. Xu M, Zhang P, Ding J, Chen J, Huo L, Liu Z. Albumin binder-conjugated fibroblast activation protein inhibitor radiopharmaceuticals for cancer therapy. *J Nucl Med.* (2021). doi: 10.2967/jnumed.121.262533

363. Zhang P, Xu M, Ding J, Chen J, Zhang T, Huo L, Liu Z. Fatty acid-conjugated radiopharmaceuticals for fibroblast activation protein-targeted radiotherapy. *Eur J Nucl Med Mol Imaging.* (2021). doi: 10.1007/s00259-021-05591-x. [Epub ahead of print].

364. Lin JJ, Chuang CP, Lin JY, Huang FT, Huang CW. Rational design, pharmacomodulation, and synthesis of [68 Ga]Ga-Alb-FAPtp-01, a selective tumor-associated fibroblast activation protein tracer for PET imaging of glioma. *ACS Sensors.* (2021) 6:3424–35. doi: 10.1021/acssensors.1c01316

365. Zhao L, Niu B, Fang J, Pang Y, Li S, Xie C, et al. Synthesis, preclinical evaluation, and a pilot clinical PET imaging study of 68 Ga-labeled FAPI dimer. *J Nucl Med.* (2021) 49:1985–96. doi: 10.2967/jnumed.121.263016

366. Toms J, Kogler J, Maschauer S, Daniel C, Schmidkonz C, Kuwert T, et al. Targeting fibroblast activation protein: radiosynthesis and preclinical evaluation of an 18 F-labeled FAP inhibitor. *J Nucl Med.* (2020) 61:1806–13. doi: 10.2967/jnumed.120.242958

367. Wang S, Zhou X, Xu X, Ding J, Liu S, Hou X, et al. Clinical translational evaluation of Al 18 F-NOTA-FAPI for fibroblast activation protein-targeted tumour imaging. *Eur J Nucl Med Mol Imaging.* (2021) 48:4259–71. doi: 10.1007/s00259-021-05470-5

368. Hicks RJ, Roselt PJ, Kallur KG, Tothill RW, Mileshkin L, FAPI. PET/CT: will it end the hegemony of 18F-FDG in oncology? *J Nucl Med.* (2021) 62:296–302. doi: 10.2967/jnumed.120.256271

369. Dorst DN, Rijpkema M, Buitinga M, Walgreen B, Helsen MMA, Brennan E, et al. Targeting of fibroblast activation protein in rheumatoid arthritis patients: imaging and *ex vivo* photodynamic therapy. *Rheumatology.* (2021). doi: 10.1093/rheumatology/keab664. [Epub ahead of print].

370. Nahrendorf M, Keliher E, Panizzi P, Zhang H, Hembrador S, Figueiredo JL, et al. 18F-4V for PET-CT imaging of VCAM-1 expression in atherosclerosis. *JACC Cardiovasc Imaging.* (2009) 2:1213–22. doi: 10.1016/j.jcmg.2009.04.016

371. Bala G, Blykers A, Xavier C, Descamps B, Broisat A, Ghezzi C, et al. Targeting of vascular cell adhesion molecule-1 by 18F-labelled nanobodies for PET/CT imaging of inflamed atherosclerotic plaques. *Eur Hear journal Cardiovasc Imaging.* (2016) 17:1001–8. doi: 10.1093/ehjci/jev346

372. Zhang X, Liu C, Hu F, Zhang Y, Wang J, Gao Y, et al. Imaging of VCAM-1 expression and monitoring therapy response in tumor with a 68 Ga-labeled single chain variable fragment. *Mol Pharm.* (2018) 15:609–18. doi: 10.1021/acs.molpharmaceut.7b00961

373. Pastorino S, Baldassari S, Ailuno G, Zuccari G, Drava G, Petretto A, et al. Two novel PET radiopharmaceuticals for endothelial vascular cell adhesion molecule-1 (VCAM-1) Targeting. *Pharmaceutics.* (2021) 13:1025. doi: 10.3390/pharmaceutics13071025

374. Golestani R, Mirfeizi L, Zeebregts CJ, Westra J, de Haas HJ, Glaudemans AWJM, et al. Feasibility of [18F]-RGD for ex vivo imaging of atherosclerosis in detection of αvβ3 integrin expression. *J Nucl Cardiol.* (2015) 22:1179–86. doi: 10.1007/s12350-014-0061-8

375. Ebenhan T, Kleynhans J, Zeevaart JR, Jeong JM, Sathekge M. Non-oncological applications of RGD-based single-photon emission tomography and positron emission tomography agents. *Eur J Nucl Med Mol Imaging.* (2021) 48:1414–33. doi: 10.1007/s00259-020-04975-9

376. Liolios C, Sachpekidis C, Kolocouris A, Dimitrakopoulou-Strauss A, Bouziotis P. PET diagnostic molecules utilizing multimeric cyclic RGD peptide analogs for imaging integrin αvβ3 receptors. *Molecules.* (2021) 26:1792. doi: 10.3390/molecules26061792

377. Hoshiga M, Alpers CE, Smith LL, Giachelli CM, Schwartz SM. αvβ3 integrin expression in normal and atherosclerotic artery. *Circ Res.* (1995) 77:1129–35. doi: 10.1161/01.RES.77.6.1129

378. Beer AJ, Pelisek J, Heider P, Saraste A, Reeps C, Metz S, et al. PET/CT imaging of integrin αvβ3 expression in human carotid atherosclerosis. *JACC Cardiovasc Imaging.* (2014) 7:178–87. doi: 10.1016/j.jcmg.2013.12.003

379. Steiger K, Quigley NG, Groll T, Richter F, Zierke MA, Beer AJ, et al. There is a world beyond αvβ3-integrin: Multimeric ligands for imaging of the integrin subtypes αvβ6, αvβ8, αvβ3, and α5β1 by positron emission tomography. *EJNMMI Res.* (2021) 11:106. doi: 10.1186/s13550-021-00842-2

380. Iqbal N, Iqbal N. Human epidermal growth factor receptor 2 (HER2) in cancers: overexpression and therapeutic implications. *Mol Biol Int.* (2014) 2014:1–9. doi: 10.1155/2014/852748

381. Tamura K, Kurihara H, Yonemori K, Tsuda H, Suzuki J, Kono Y, et al. 64Cu-DOTA-trastuzumab PET imaging in patients with HER2-positive breast cancer. *J Nucl Med.* (2013) 54:1869–75. doi: 10.2967/jnumed.112.118612

382. Baum RP, Prasad V, Müller D, Schuchardt C, Orlova A, Wennborg A, et al. Molecular imaging of HER2-expressing malignant tumors in breast cancer patients using synthetic 111In- or 68Ga-labeled affibody molecules. *J Nucl Med.* (2010) 51:892–7. doi: 10.2967/jnumed.109.073239

383. Dijkers EC, Oude Munnink TH, Kosterink JG, Brouwers AH, Jager PL, De Jong JR, et al. Biodistribution of 89Zr-trastuzumab and PET imaging of HER2-positive lesions in patients with metastatic breast cancer. *Clin Pharmacol Ther.* (2010) 87:586–92. doi: 10.1038/clpt.2010.12

384. Gebhart G, Lamberts LE, Wimana Z, Garcia C, Emonts P, Ameye L, et al. Molecular imaging as a tool to investigate heterogeneity of advanced HER2-positive breast cancer and to predict patient outcome under trastuzumab emtansine (T-DM1): the ZEPHIR trial. *Ann Oncol.* (2016) 27:619–24. doi: 10.1093/annonc/mdv577

385. Pereira PMR, Norfleet J, Lewis JS, Escorcia FE. Immuno-PET detects changes in multi-RTK tumor cell expression levels in response to targeted kinase inhibition. *J Nucl Med.* (2021) 62:366. doi: 10.2967/jnumed.120.244897

386. Veronese M, Santangelo B, Jauhar S, D'Ambrosio E, Demjaha A, Salimbeni H, et al. A potential biomarker for treatment stratification in psychosis: evaluation of an [18F] FDOPA PET imaging approach. *Neuropsychopharmacol.* (2020) 46:1122–32. doi: 10.1038/s41386-020-00866-7

387. van der Geest KSM, Sandovici M, van Sleen Y, Sanders JS, Bos NA, Abdulahad WH, et al. Review: what is the current evidence for disease subsets in giant cell arteritis? *Arthritis Rheumatol.* (2018) 70:1366. doi: 10.1002/art.40520

388. Signore A, Annovazzi A, Barone R, Bonanno E, D'Alessandria C, Chianelli M, et al. 99mTc-interleukin-2 scintigraphy as a potential tool for evaluating tumor-infiltrating lymphocytes in melanoma lesions: a validation study. *J Nucl Med.* (2004) 45:1647–52.

389. van Sleen Y, Sandovici M, Abdulahad WH, Bijzet J, van der Geest KSM, Boots AMH, et al. Markers of angiogenesis and macrophage products for predicting disease course and monitoring vascular inflammation in giant cell arteritis. *Rheumatology.* (2019) 58:1383–92. doi: 10.1093/rheumatology/kez034

390. Cid MC, Unizony SH, Blockmans D, Brouwer E, Dagna L, Dasgupta B, et al. Efficacy and safety of mavrilimumab in giant cell arteritis: a phase 2, randomised, double-blind, placebo-controlled trial. *Ann Rheum Dis.* (2022) 81:653–61. doi: 10.1136/annrheumdis-2021-221865

391. Eichendorff S, Svendsen P, Bender D, Keiding S, Christensen EI, Deleuran B, et al. Biodistribution and PET imaging of a novel [68Ga]-anti-CD163-antibody conjugate in rats with collagen-induced arthritis and in controls. *Mol Imaging Biol.* (2015) 17:87–93. doi: 10.1007/s11307-014-0768-6

392. Fu R, Carroll L, Yahioglu G, Aboagye EO, Miller PW. Antibody fragment and affibody immunoPET imaging agents: radiolabelling strategies and applications. *ChemMedChem.* (2018) 13:2466. doi: 10.1002/cmdc.201800624

393. Debie P, Devoogdt N, Hernot S. Targeted nanobody-based molecular tracers for nuclear imaging and image-guided surgery. *Antibodies.* (2019) 8:12. doi: 10.3390/antib8010012

394. Pascali G, Matesic L. How Far Are We from Dose On Demand of Short-Lived Radiopharmaceuticals? *Perspect Nucl Med Mol Diagnosis Integr Ther.* (2016) 79–92. doi: 10.1007/978-4-431-55894-1_6

395. Hansen SB, Bender D. Advancement in production of radiotracers. *Semin Nucl Med.* (2021) 52:266–75. doi: 10.1053/j.semnuclmed.2021.10.003